TRANSMUTATION OF MINOR ACTINIDES IN A CANDU THORIUM BURNER

Sümer ŞAHİN

Şenay YALÇIN,Hacı Mehmet ŞAHİN,

Adem Acır,Kadir YILDIZ, Necmettin ŞAHİN

Taner ALTINOK,Mahmut ALKAN

E-mail: sumer@gazi.edu.tr

Web-page: http://w3.gazi.edu.tr/~sumer

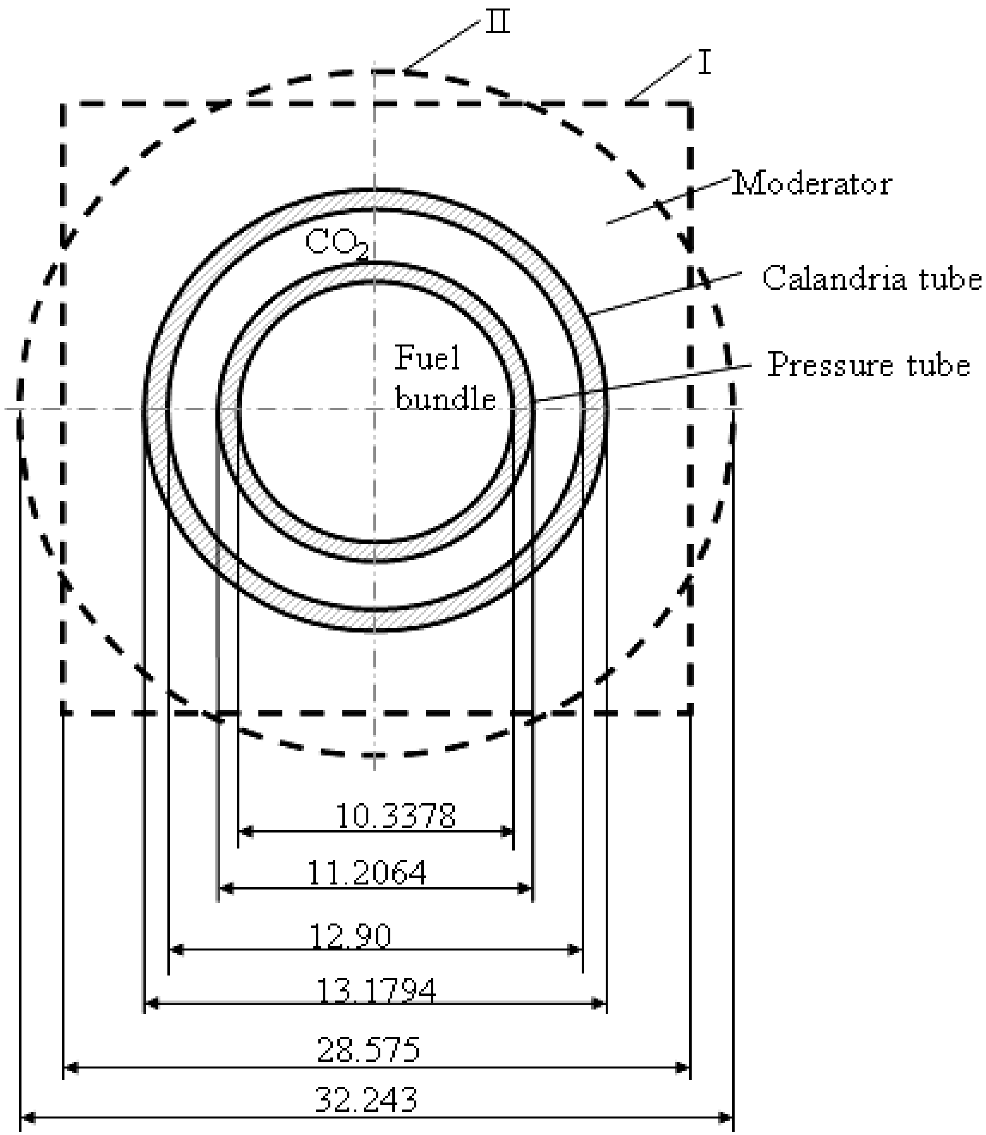

Fig. 1. Cross sectional view of the fuel channel

I- Original CANDU square lattice cell.

II- Equivalent diameter, used in calculations.

(Dimensions are in centimeters, not in scale)

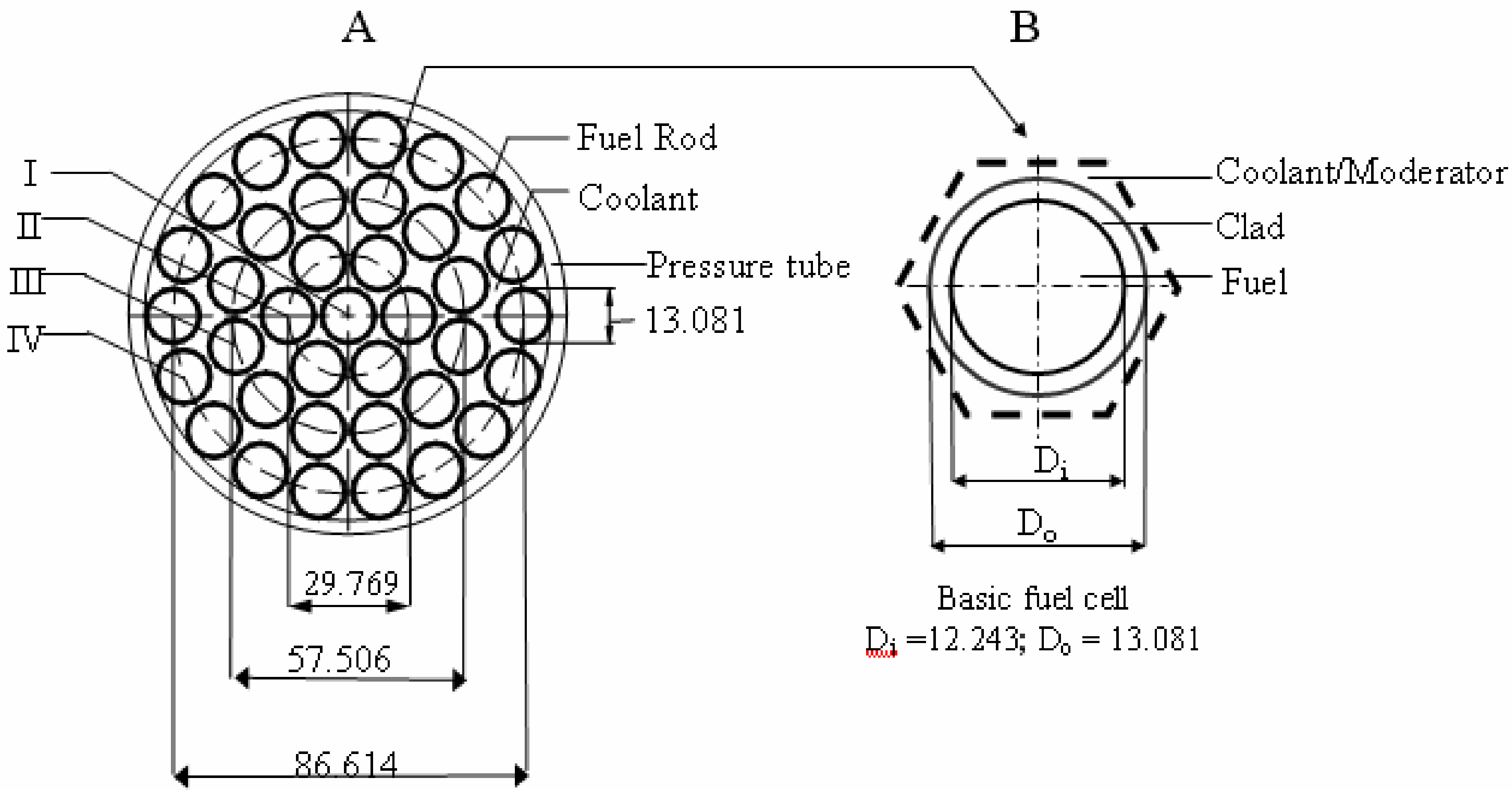

Fig. 2. Placement of 37-fuel rods in the bundle
(Dimensions are in millimeters, not in scale)

Atomic density variations in the course of breeding reactions are calculated as:

$$+\Delta N_d = \Delta t \cdot N_{m1} \int \sigma_{b,m1}(E) \cdot \Phi(E) \cdot dE + \Delta t \cdot \lambda_{m2} \cdot N_{m2} \quad (1)$$

Indices denote daughter (d) and mother (m) isotopes.

Atomic density variations in the course of depletion reactions are calculated as

$$-\Delta N = \Delta t \cdot N \cdot \int \sigma_{\mathrm{dep}}(E) \cdot \Phi(E) \cdot dE + \Delta t \cdot \lambda \cdot N \quad (2)$$

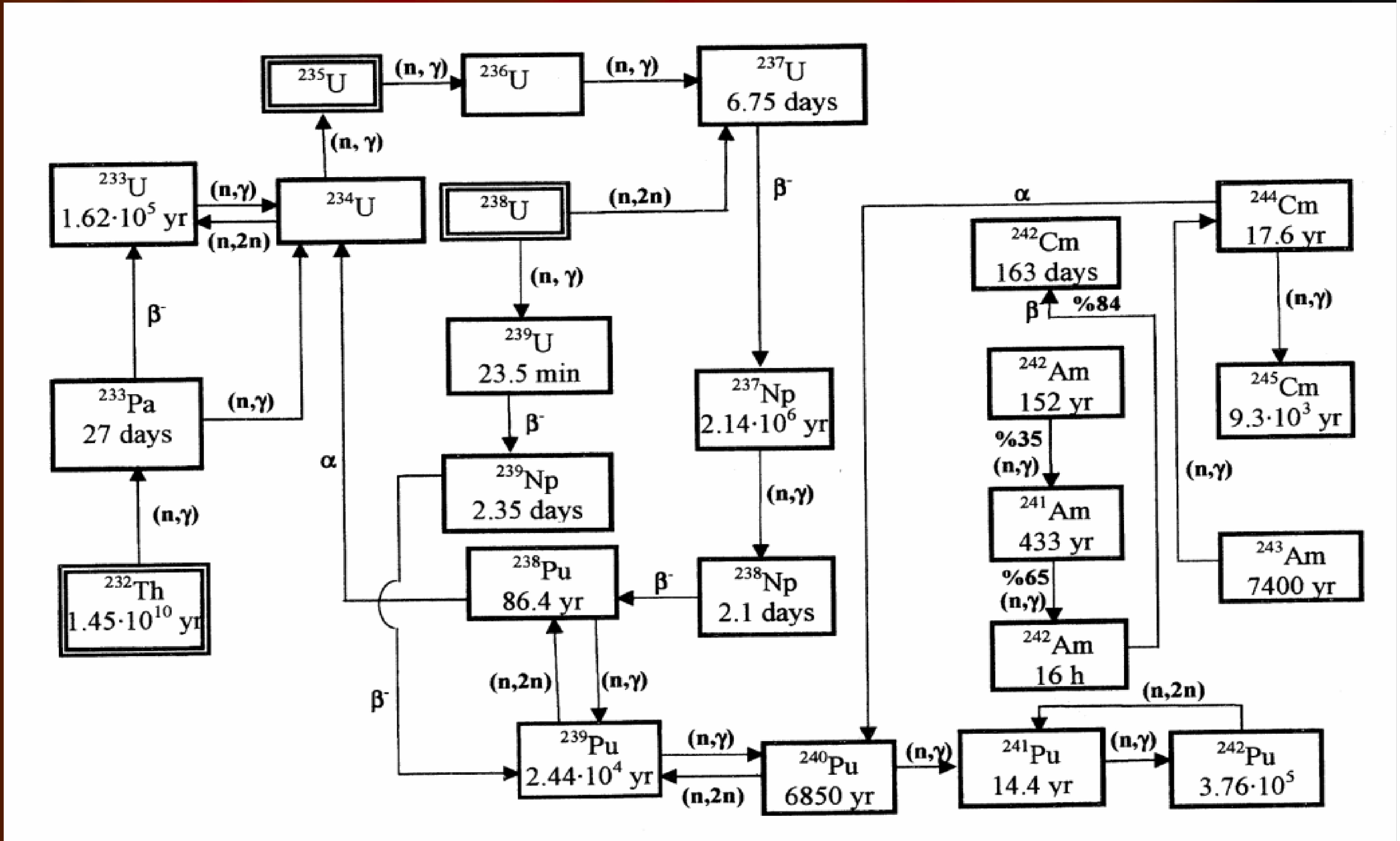

Major nuclear reactions and radioactive transformation processes in the course of reactor operation.

INCREASED FUEL BURN UP IN A CANDU THORIUM REACTOR USING REACTOR GRADE PLUTONIUM

The composition of the reactor grade plutonium]

ISOTOPES	Reactor grade plutonium initial [%]
^{238}Pu	1.0
^{239}Pu	62.0
^{240}Pu	24.0
^{241}Pu	8.0
^{242}Pu	5.0

* IAEA, 2003, Potential Of Thorium Based Fuel Cycles To Constrain Plutonium And Reduce Long Lived Waste Toxicity, IAEA-TECDOC-1349, International Atomic Energy Agency, Vienna, Austria, p.55, Table 3.3.6.

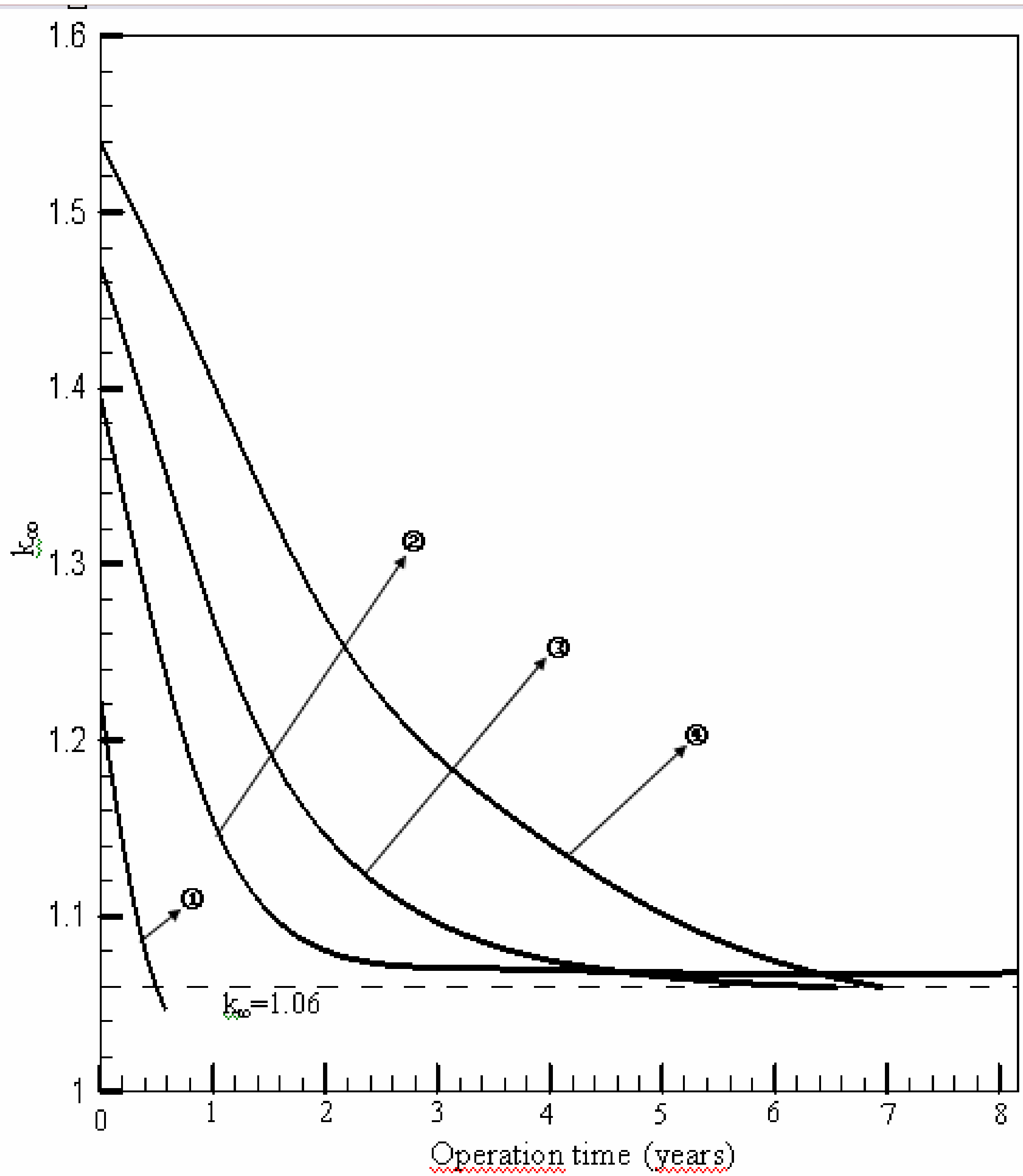

Fig. 3. Temporal variation of the lattice criticality k_∞

①:98 % ThO_2 + 2% PuO_2; ②:96 % ThO_2 + 4 % PuO_2

③:94 % ThO_2 + 6% PuO_2; ④:90 % ThO_2 + 10 % PuO_2

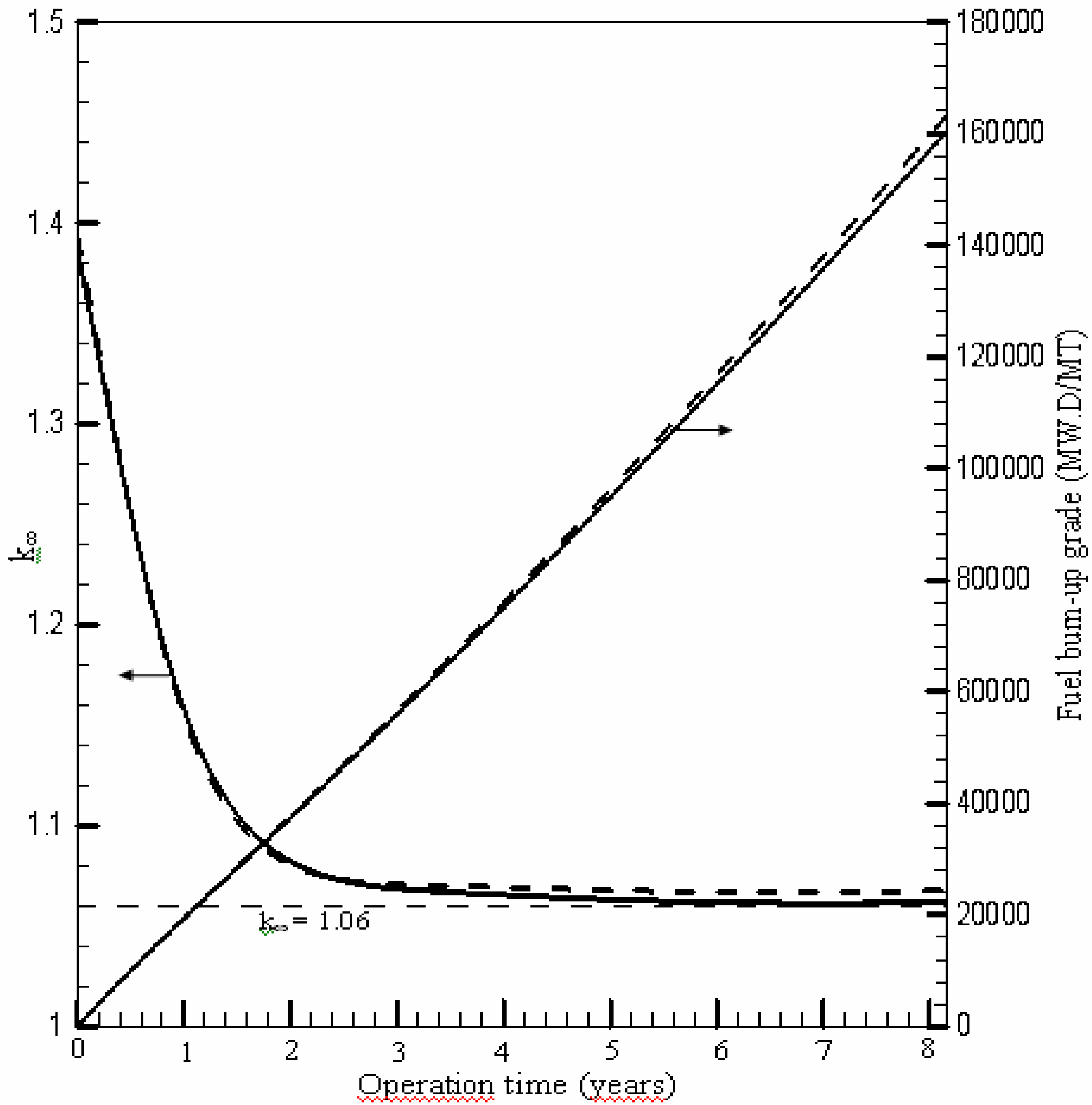

Fig. 4. Temporal variation of the lattice criticality k_∞ and the fuel burn-up grade

(Broken lines: 96 % ThO_2 + 4 % PuO_2; Solid lines: 91 % ThO_2 + 5 % UO_2 + 4 % PuO_2)

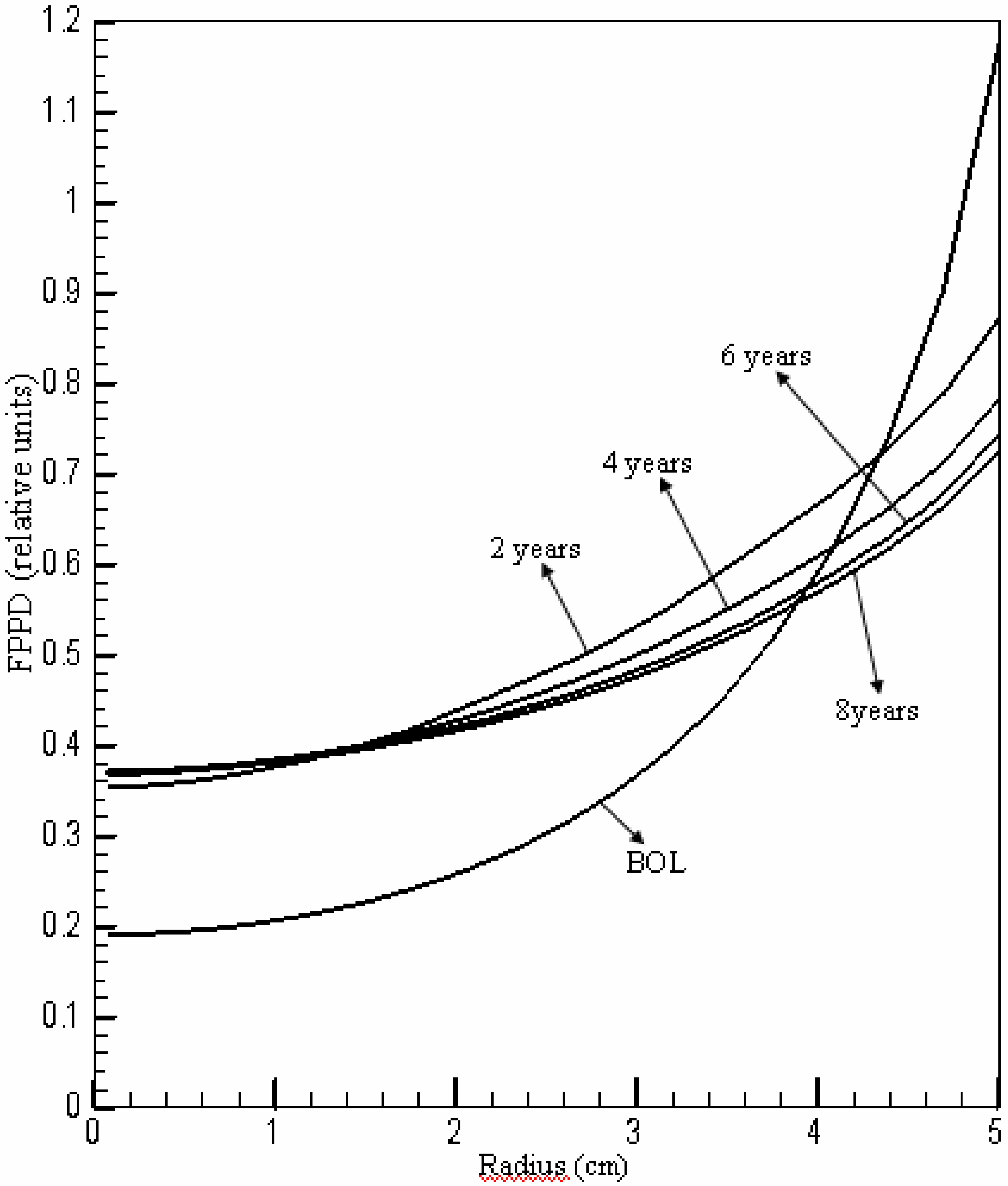

Fig. 5. The fission power production density in the fuel zone of the bundle with

91 % ThO_2 + 5 % UO_2 + 4 % PuO_2

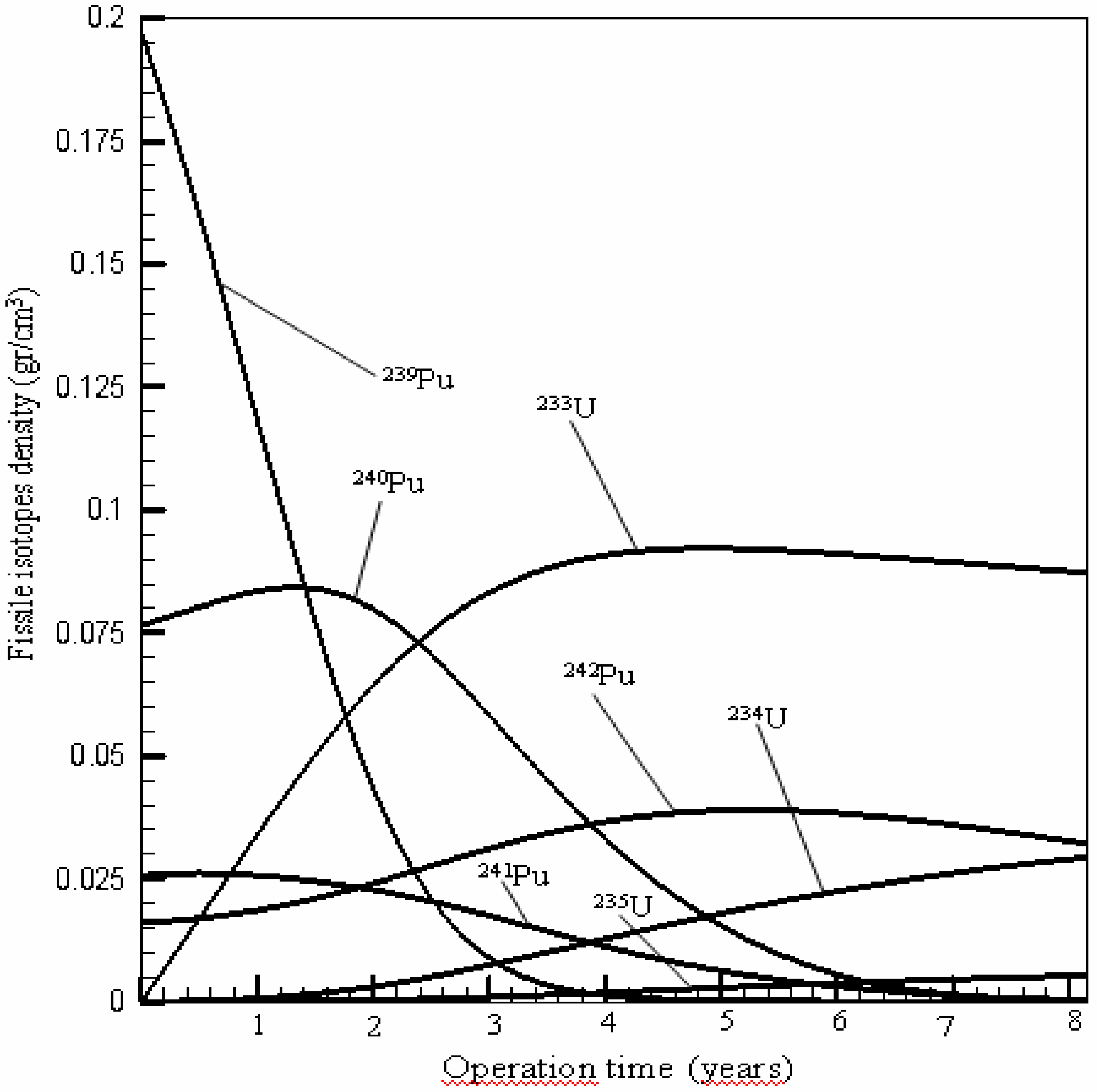

Fig. 6. Density variations of the main fissionable isotopes in the central fuel row of the bundle with 96 % ThO_2 + 4 % PuO_2

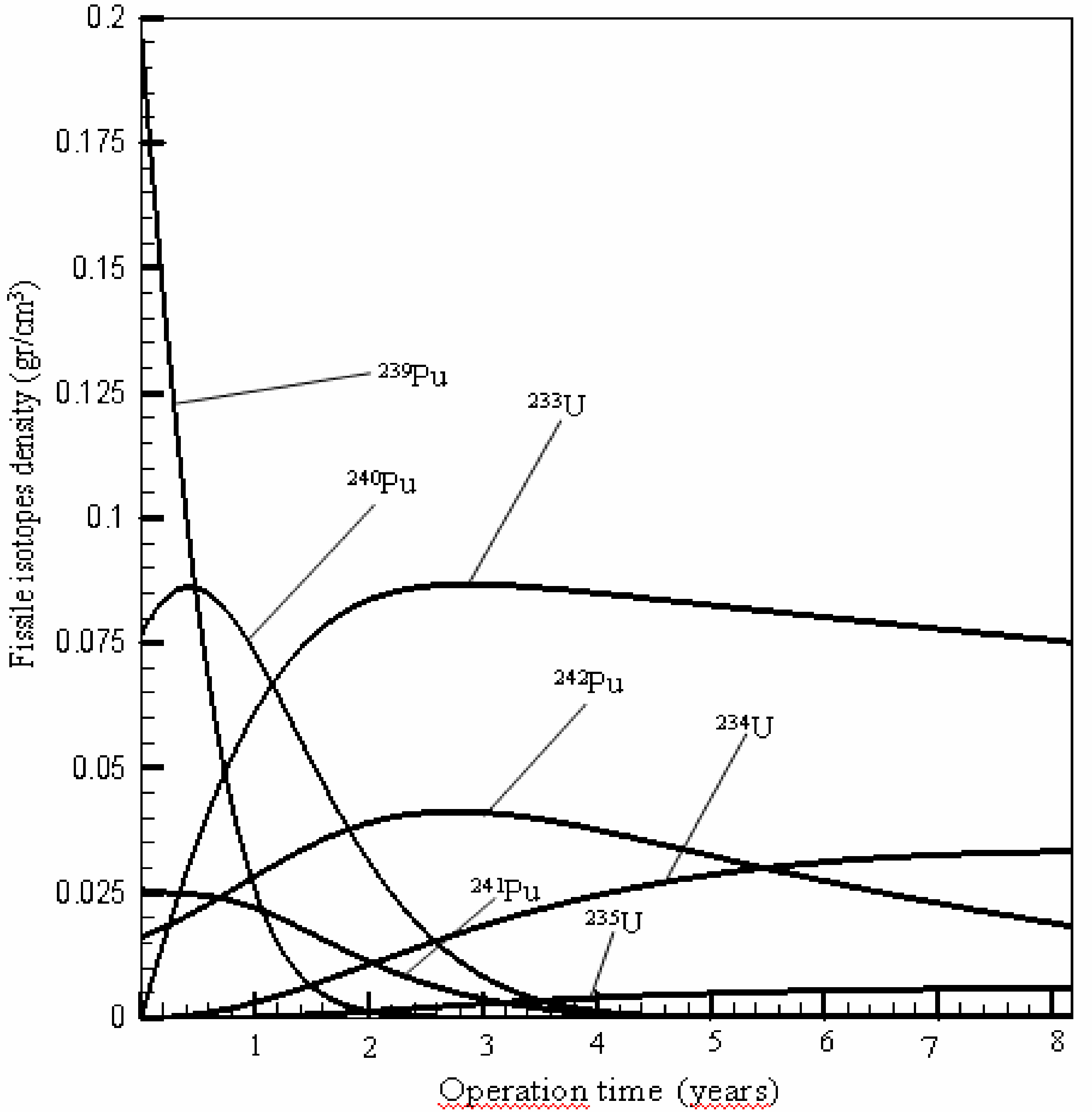

Fig. 7. Density variations of the main fissionable isotopes in the peripheral fuel row of the bundle with 96 % ThO_2 + 4 % PuO_2

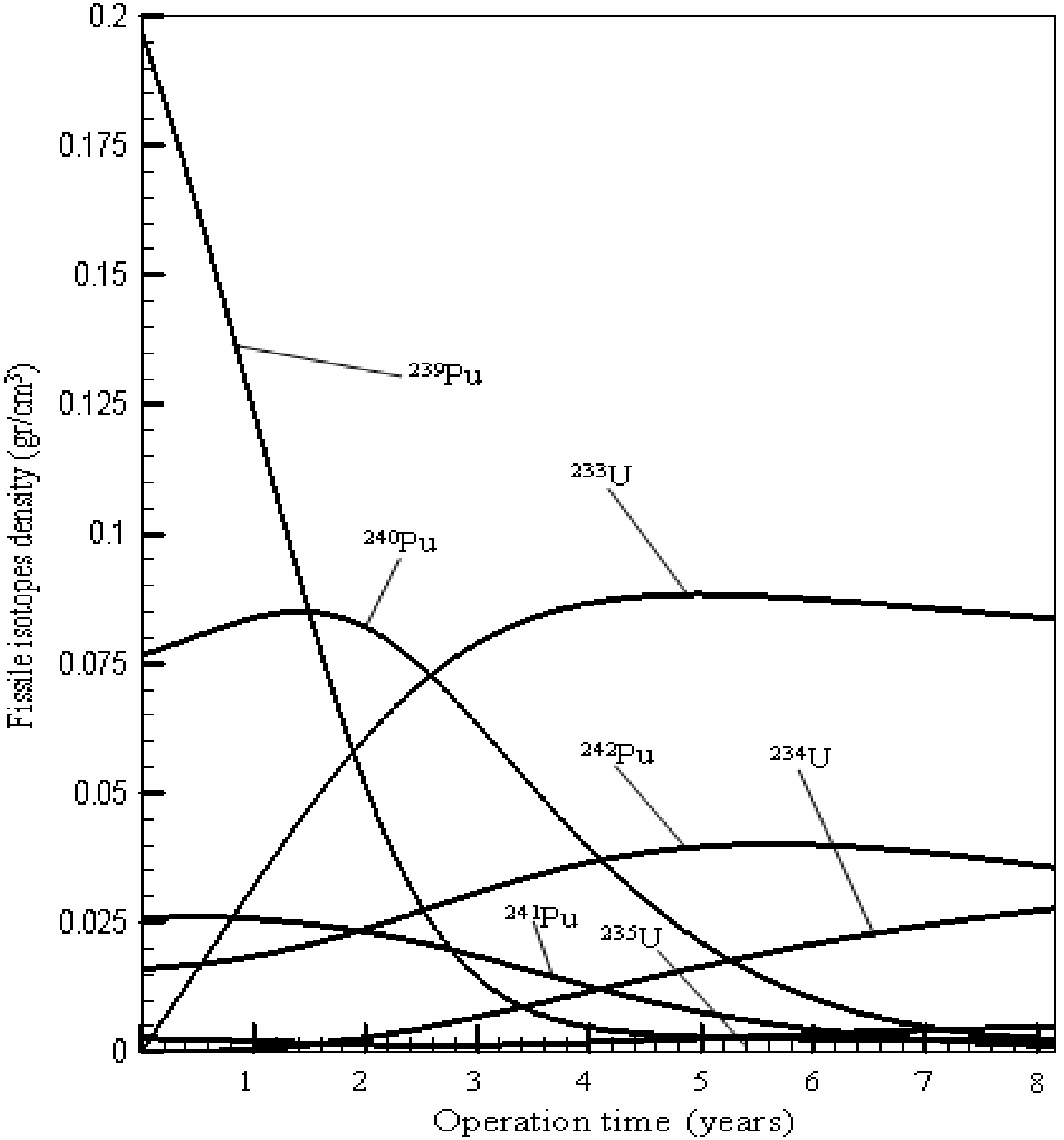

Fig. 8. Density variations of the main fissionable isotopes in the central fuel row of the bundle with 91 % ThO_2 + 5 % UO_2 + 4 % PuO_2

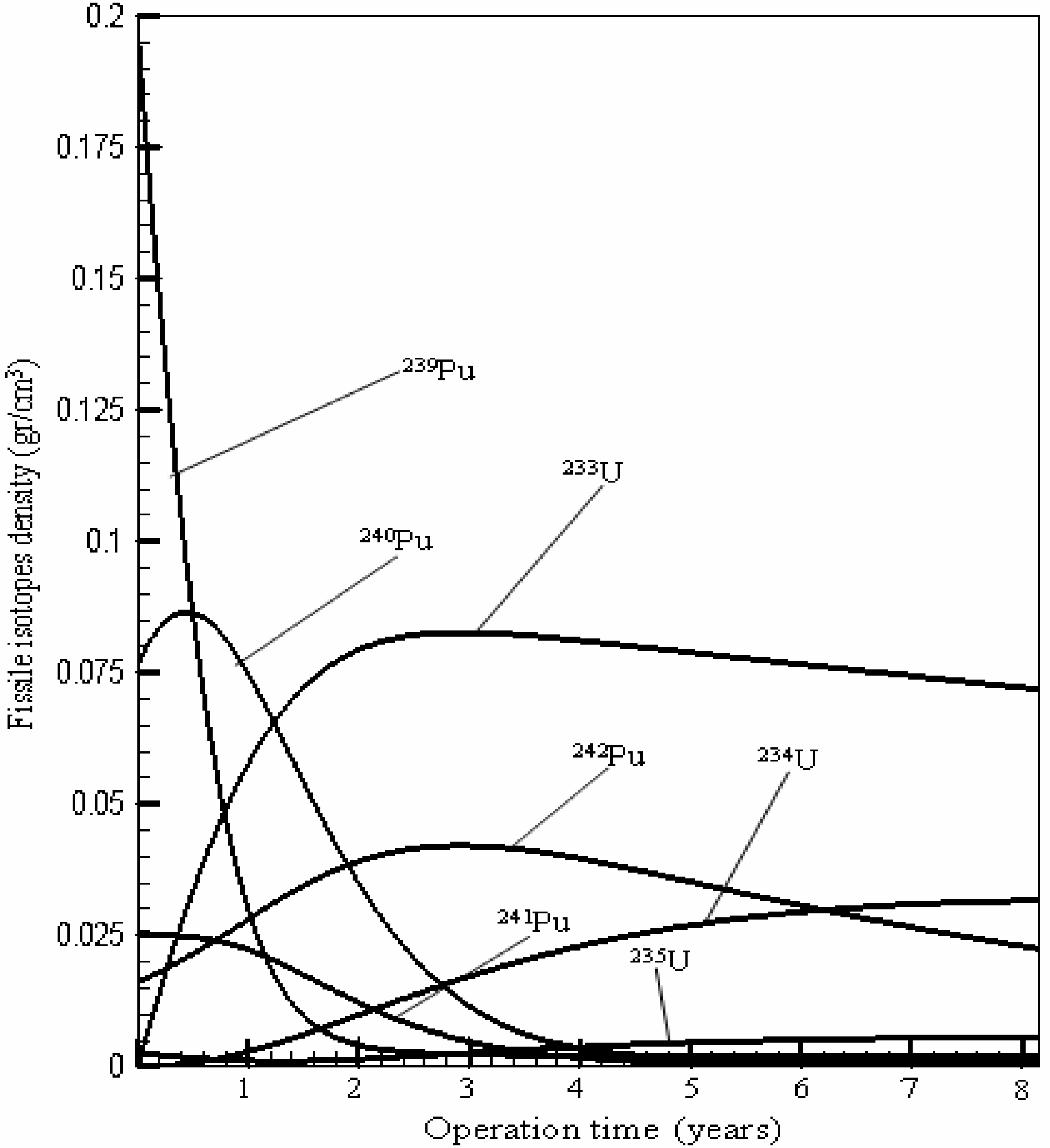

Fig. 9. Density variations of the main fissionable isotopes in the peripheral fuel row in the bundle with 91 % ThO_2 + 5 % UO_2 + 4 % PuO_2

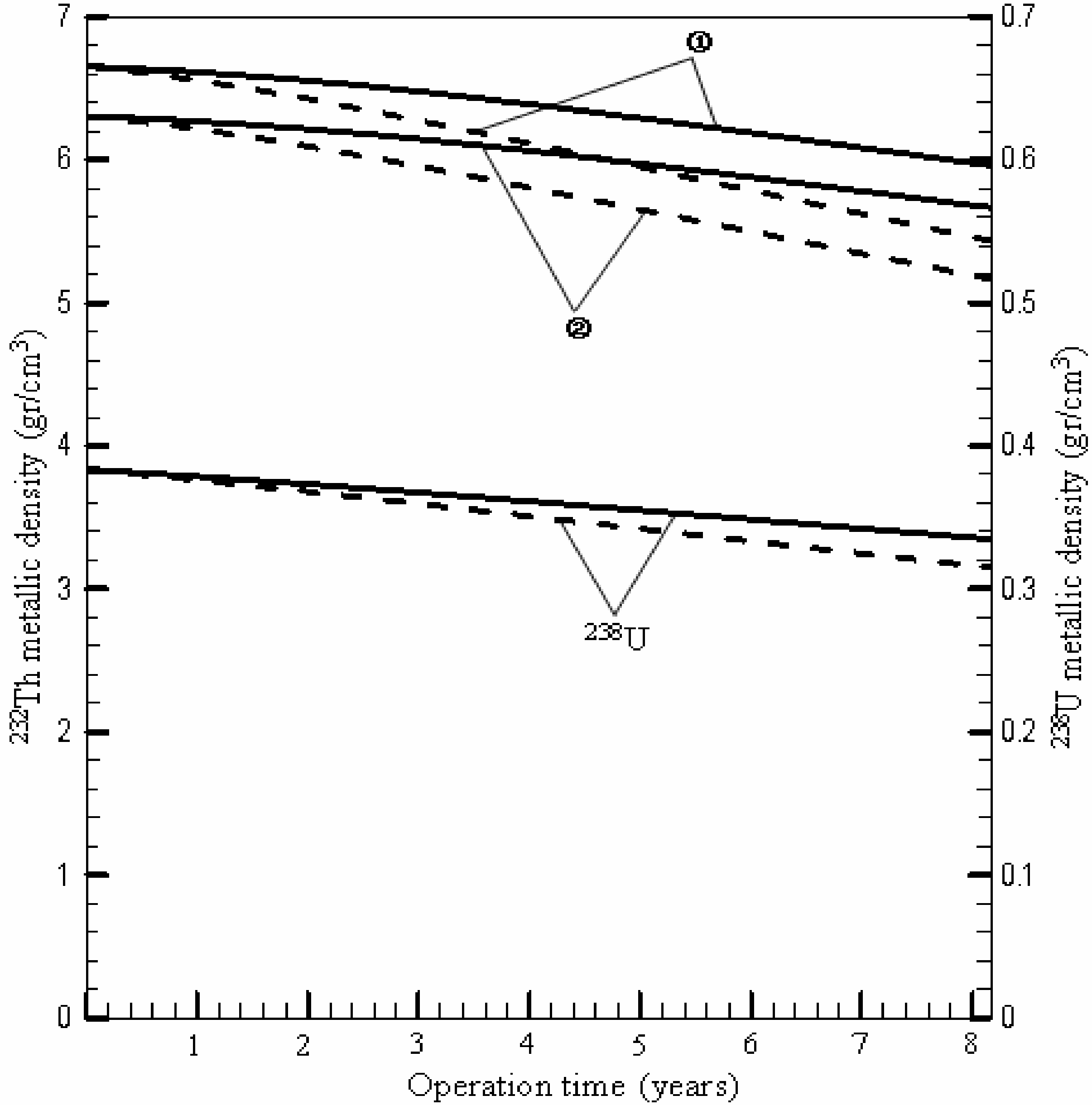

Fig. 10. Gradual depletion of the metallic density of the dominant ^{232}Th and ^{238}U isotopes

(①: 96 % ThO_2 + 4 % PuO_2; ②: 91 % ThO_2 + 5 % UO_2 + 4 % PuO_2)

(Solid lines, central fuel row; broken lines, peripheral fuel row)

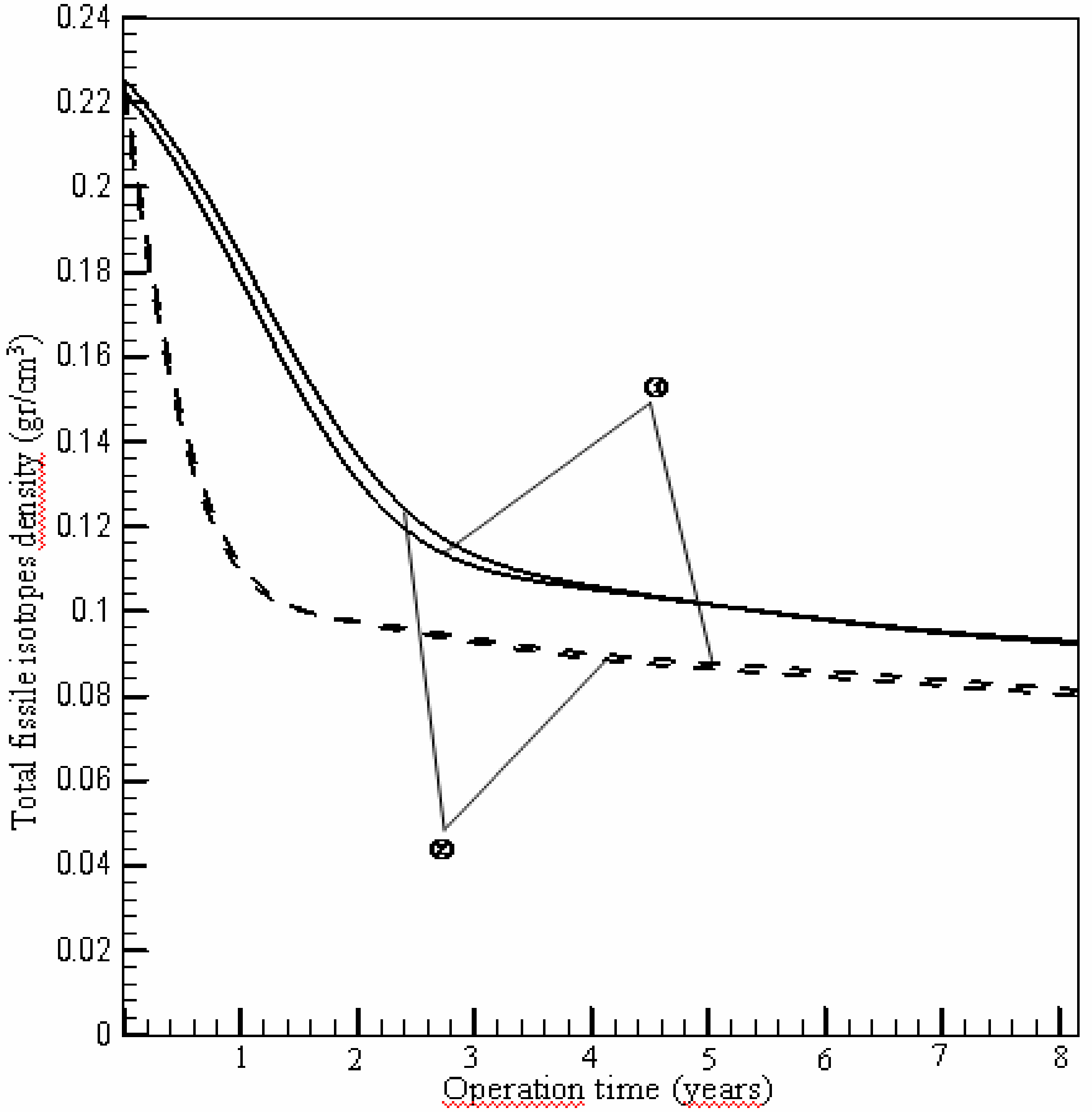

Fig. 11. Temporal variation of the accumulated densities of fissile isotopes

(^{233}U+ ^{235}U+ ^{239}Pu+ ^{241}Pu) in the fuel bundle

(Solid lines, central fuel row; broken lines, peripheral fuel row)

(① : 96 % ThO_2 + 4 % PuO_2; ② : 91 % ThO_2 + 5 % UO_2 + 4 % PuO_2)

INCREASED FUEL BURN UP IN A CANDU THORIUM REACTOR USING WEAPON GRADE PLUTONIUM

The composition of the weapon grade plutonium

ISOTOPES	Weapon grade plutonium initial [%]
^{239}Pu	94.0
^{240}Pu	6.0

* IAEA, 2003, Potential Of Thorium Based Fuel Cycles To Constrain Plutonium And Reduce Long Lived Waste Toxicity, IAEA-TECDOC-1349, International Atomic Energy Agency, Vienna, Austria, p.55, Table 3.3.6.

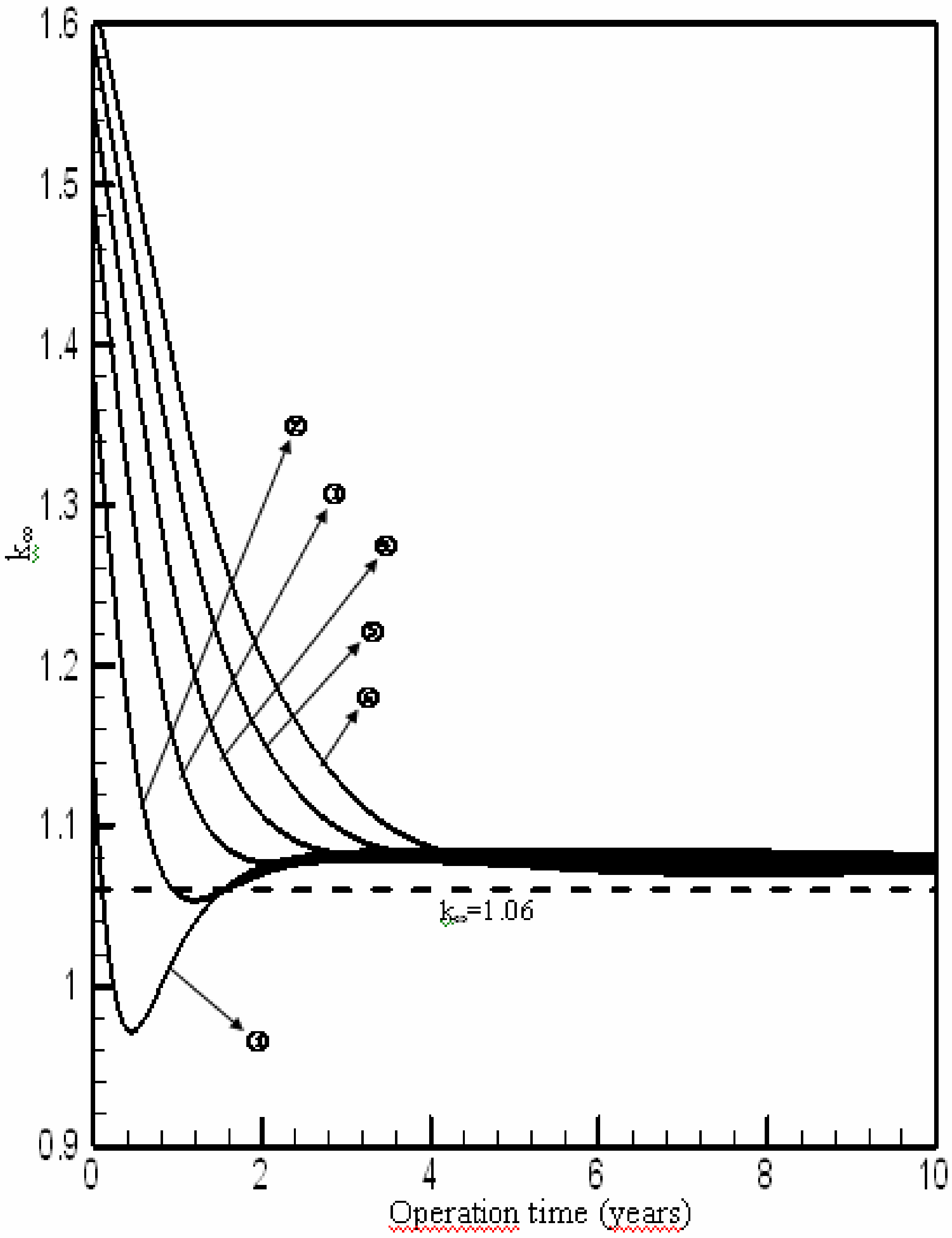

Fig. 3a. Temporal variation of the lattice criticality k_∞

❶ :99 % ThO_2 + 1 % PuO_2; ❷ :98 % ThO_2 + 2 % PuO_2; ❸ :97 % ThO_2 + 3 % PuO_2;
❹ :96 % ThO_2 + 4 % PuO_2; ❺ : 95 % ThO_2 + 5 % PuO_2; ❻ : 94 % ThO_2 + 6 % PuO_2;

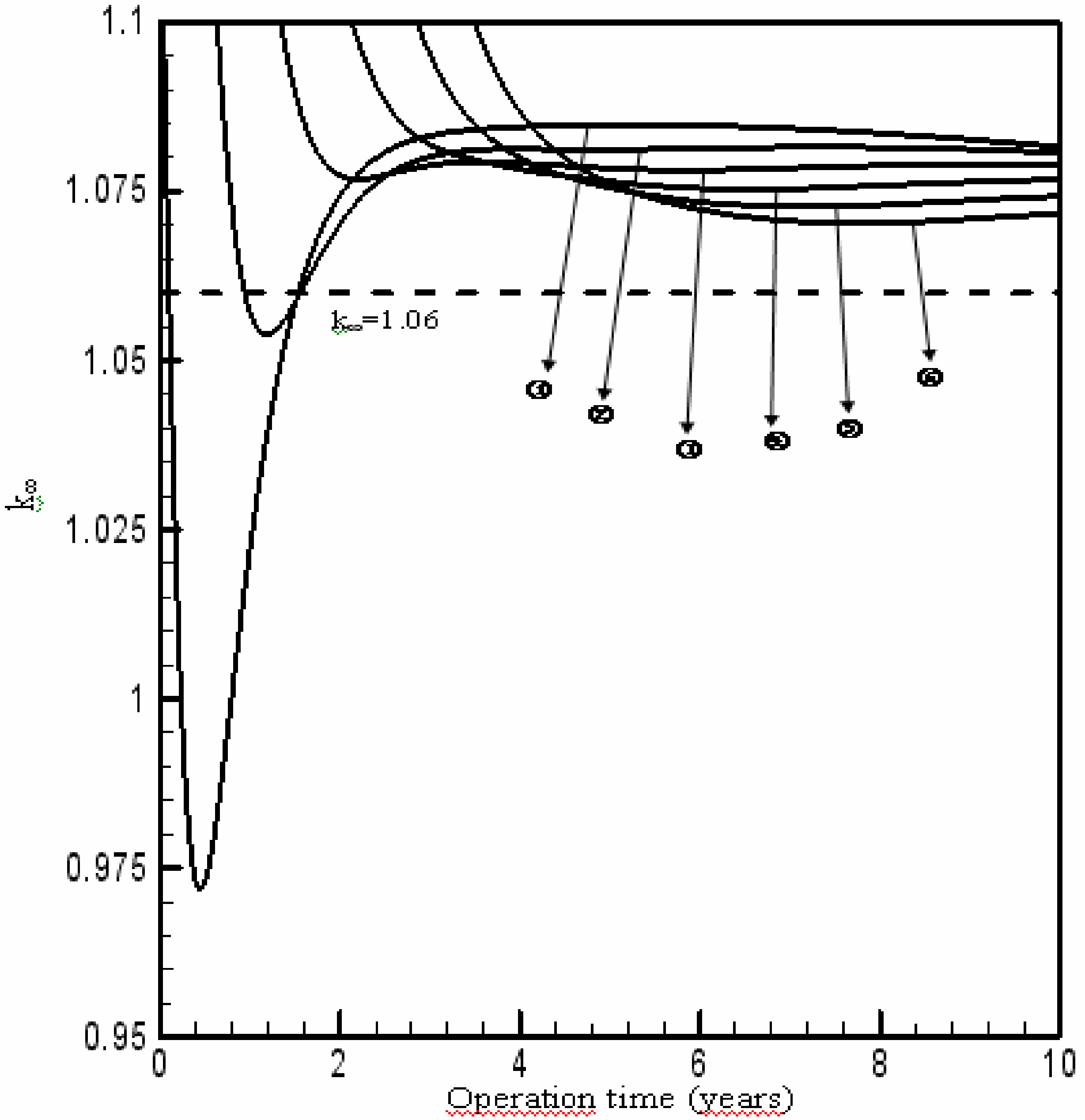

Fig.3b. Temporal variation of the lattice criticality k_∞

(Legend, as fig. 3a)

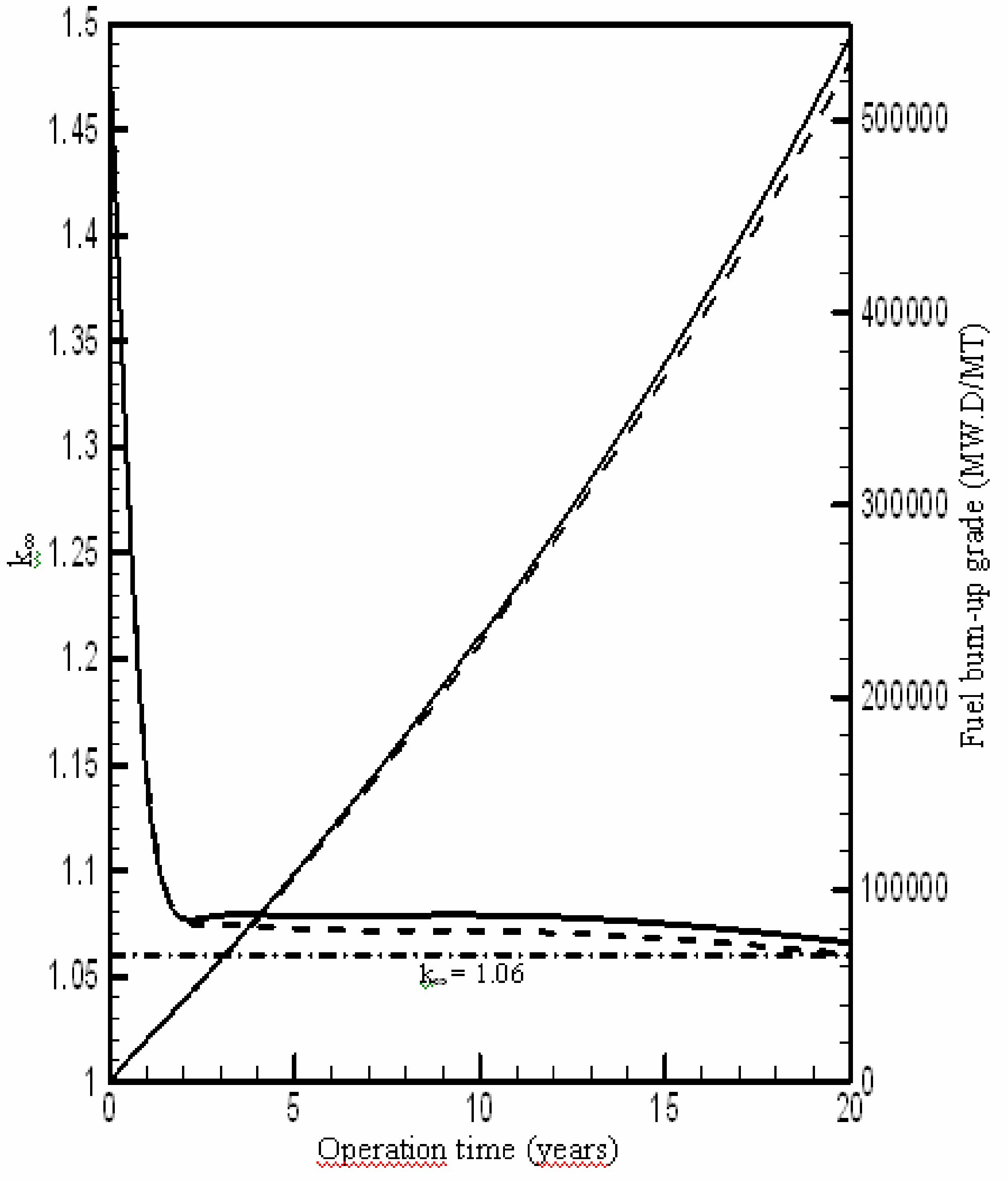

Fig. 4a. Temporal variation of the lattice criticality k_∞ and the fuel burn-up grade

(solid lines: 97 % ThO_2 + 3 % PuO_2; broken lines: 92 % ThO_2 + 5 % UO_2 + 3 % PuO_2)

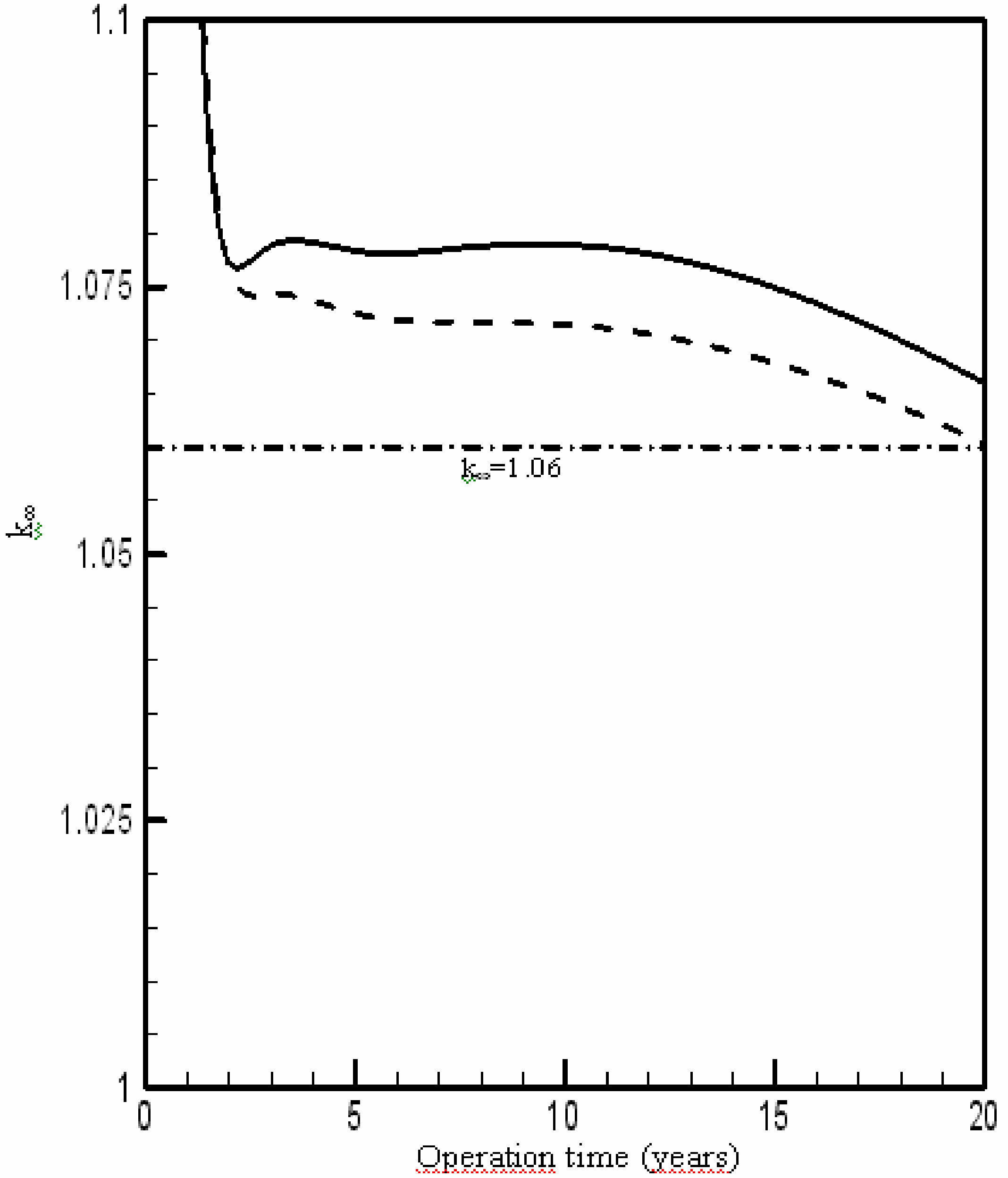

Fig. 4b. Temporal variation of the lattice criticality k_∞

(Legend, as fig. 4a)

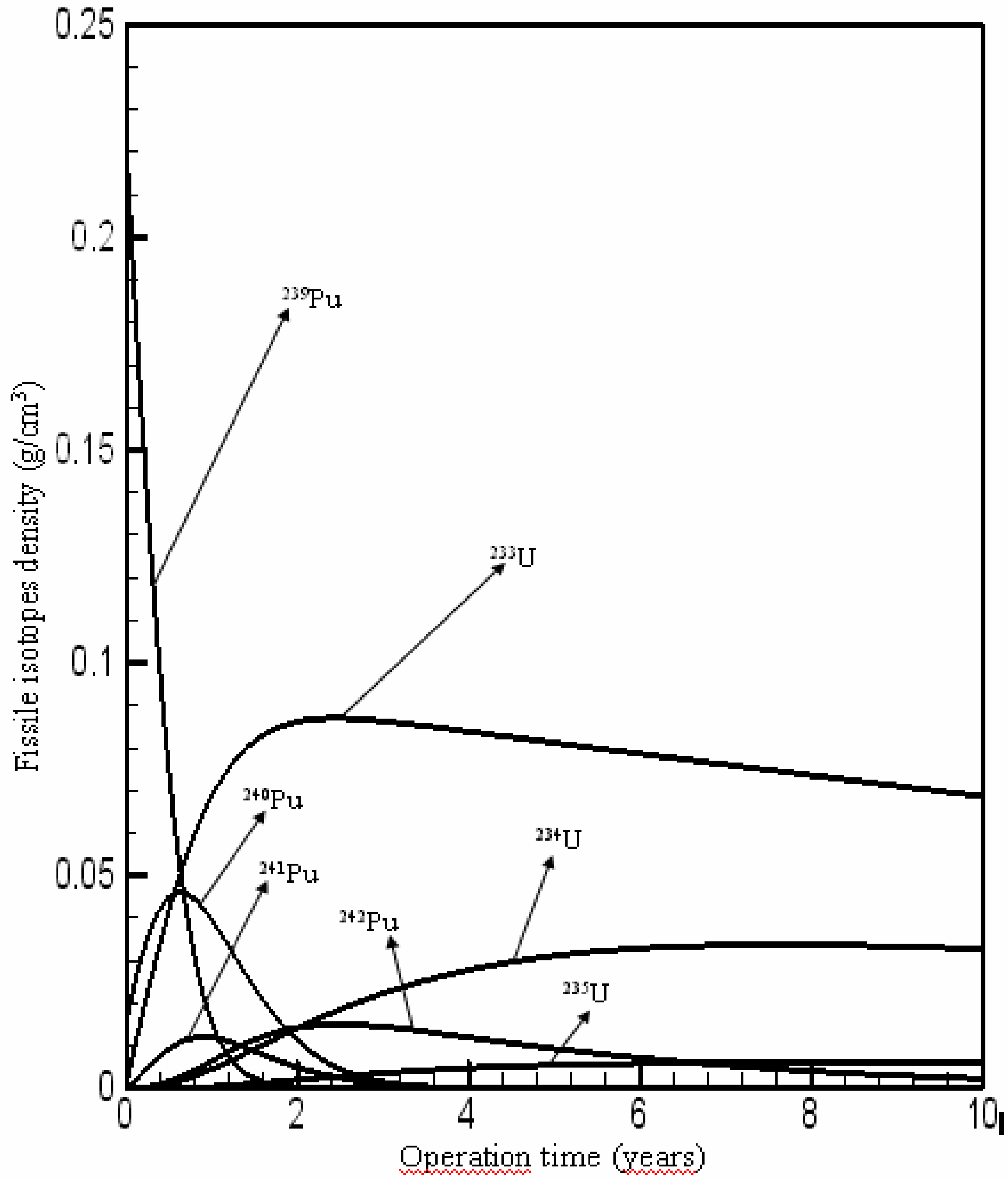

Fig. 5. Density variations of the peripheral fuel row of the main fissionable isotopes in the bundle with 97 % ThO_2 +3 % PuO_2

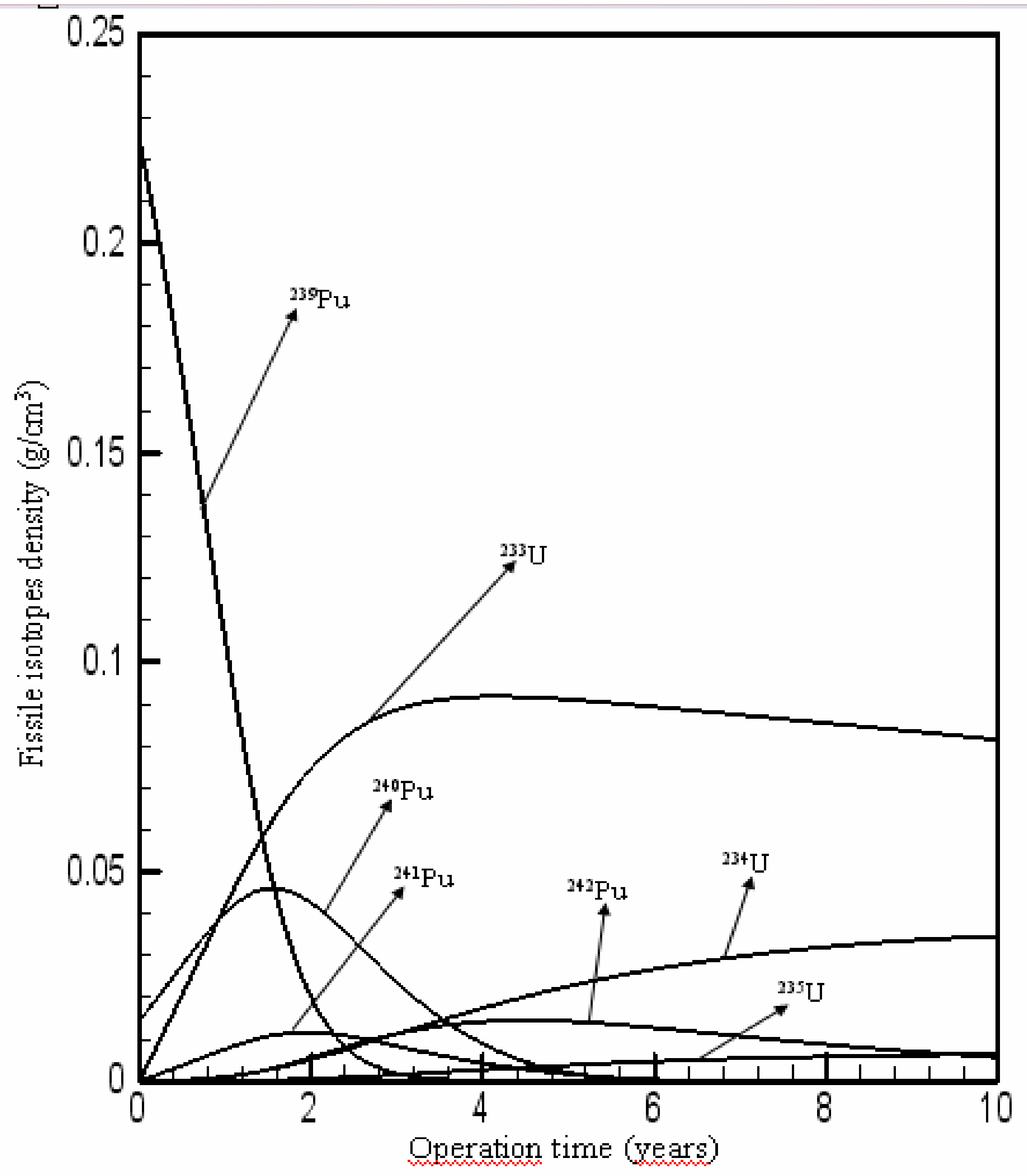

Fig. 6. Density variations of the central fuel row of the main fissionable isotopes in the bundle with 97 % ThO_2 +3 % PuO_2

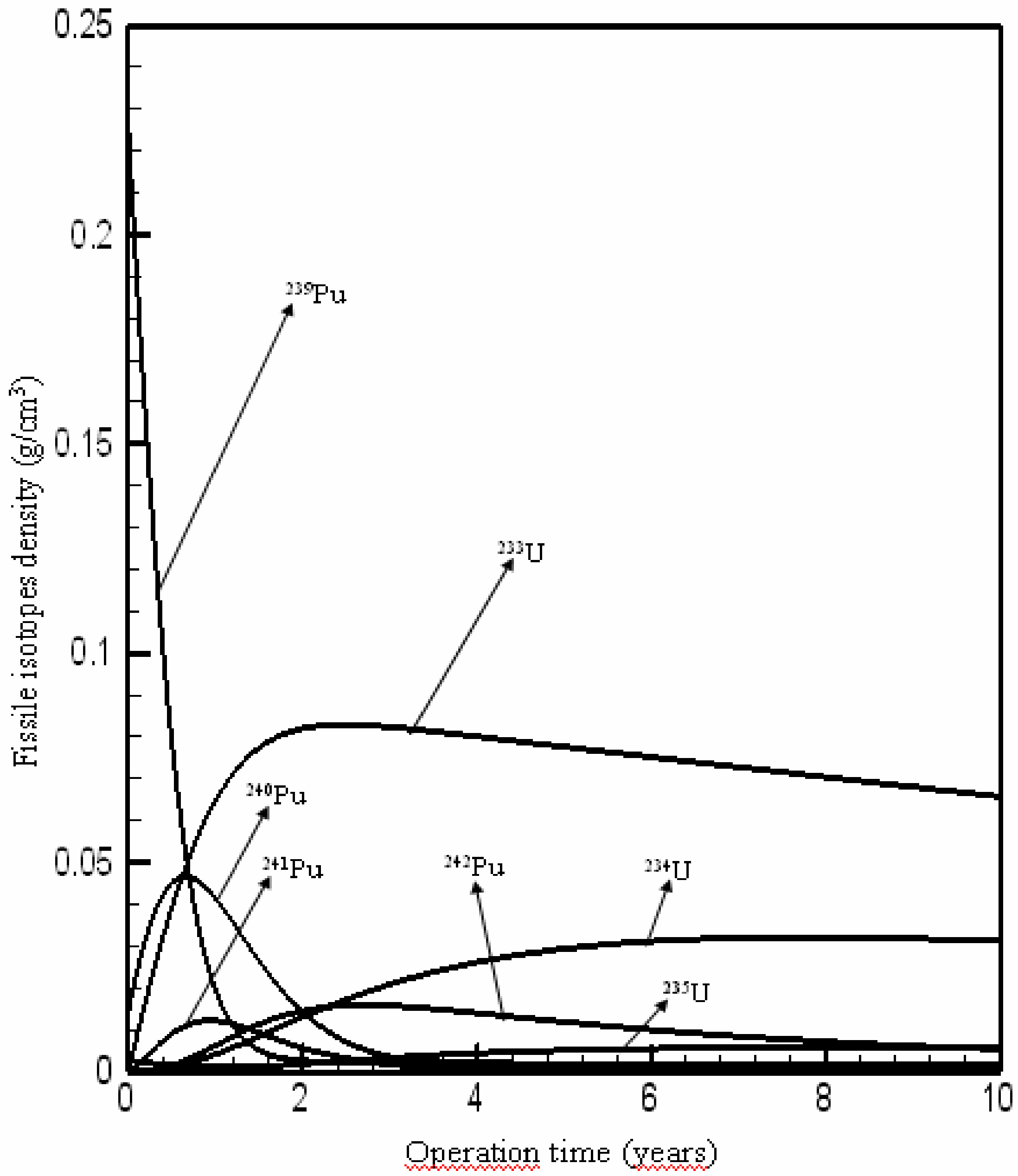

Fig. 7. Density variations of the peripheral fuel row of the main fissionable isotopes in the bundle with 92 % ThO_2 +5 % UO_2+3 % PuO_2

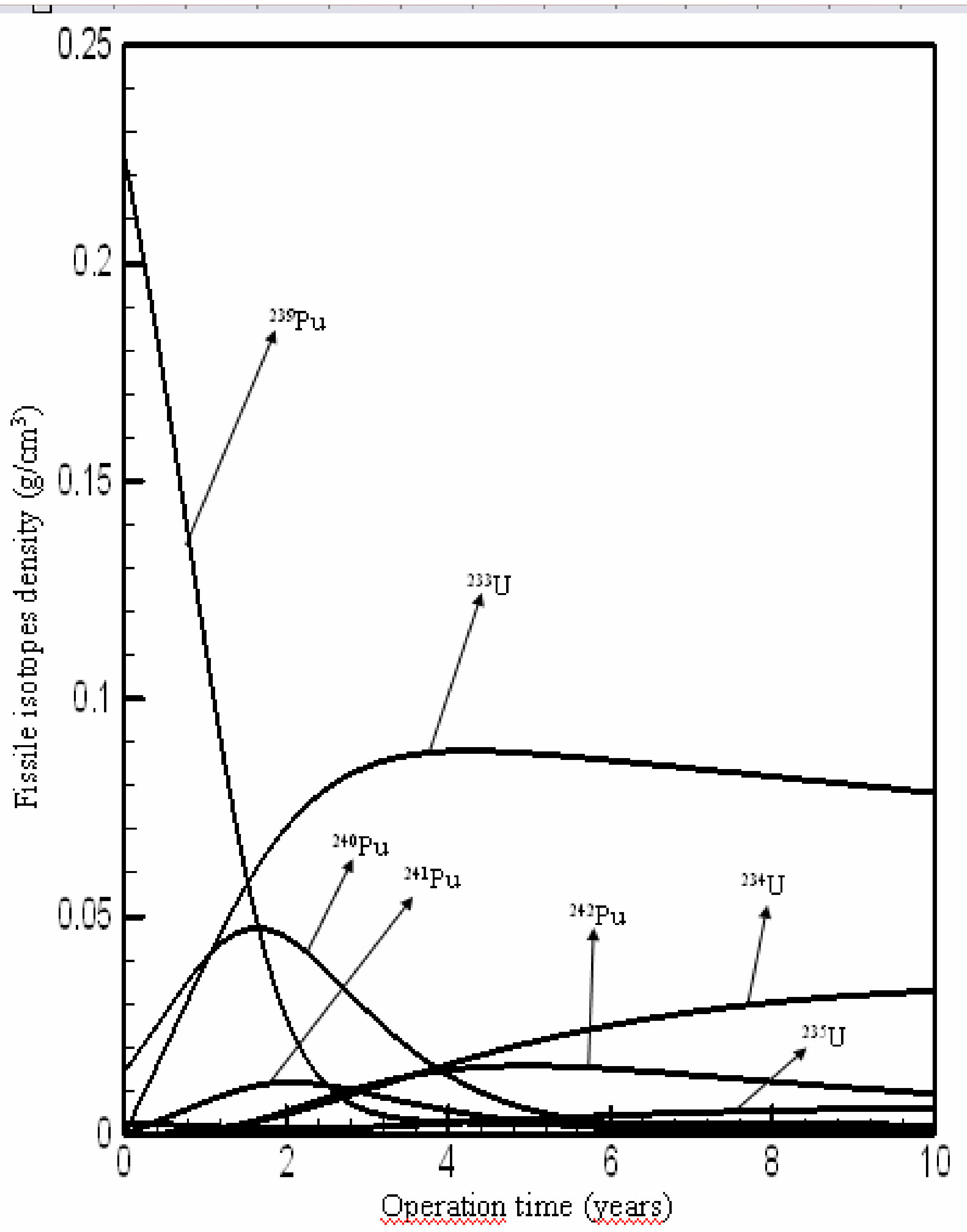

Fig. 8. Density variations of the central fuel row of the main fissionable isotopes in the bundle with 92 % ThO_2 +5 % UO_2 +3 % PuO_2

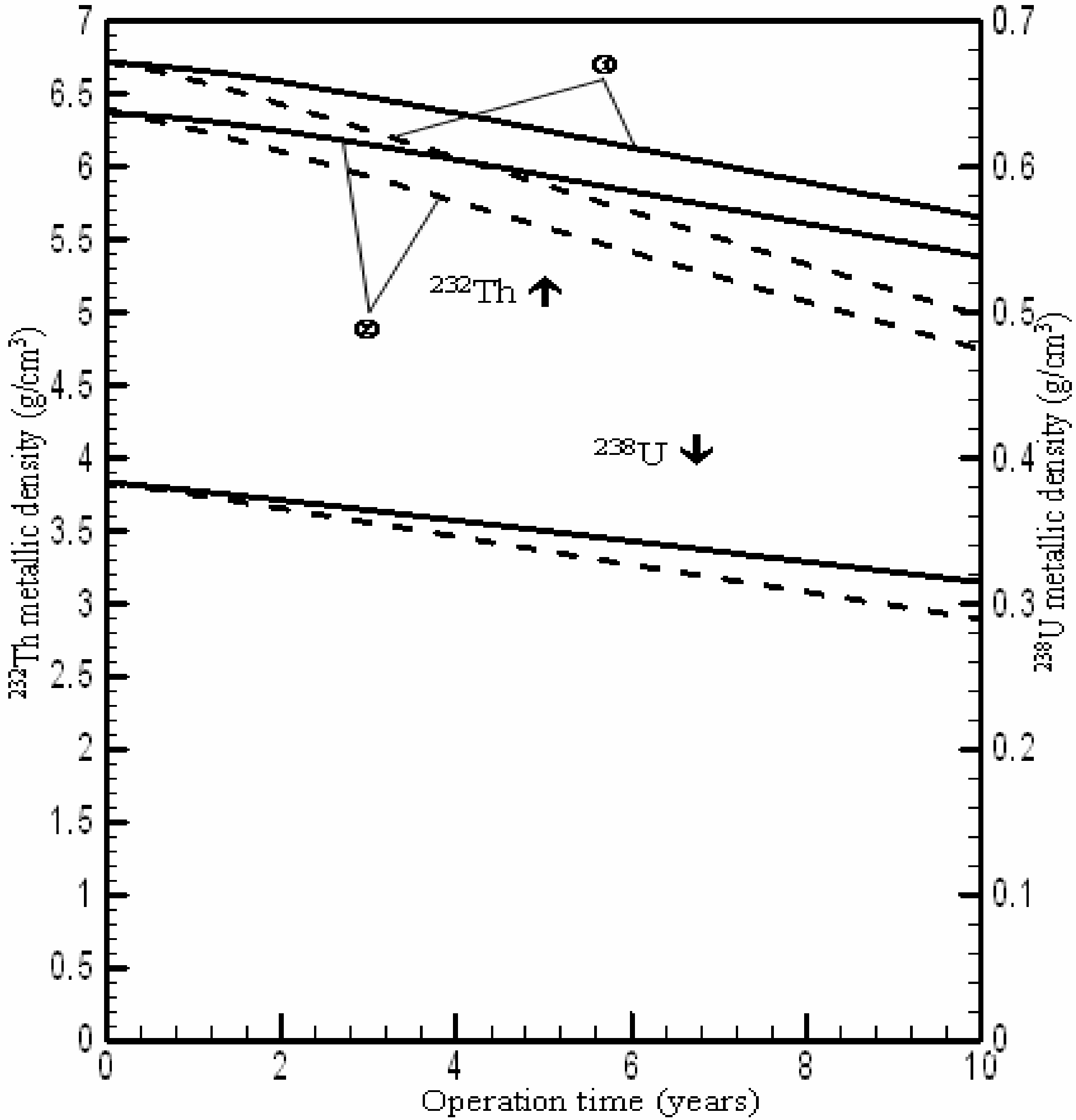

Fig. 9. Gradual depletion of the metallic density of the dominant ^{232}Th and ^{238}U isotopes

(➀ : 97 % ThO_2 + 3 % PuO_2; ➁ : 92 % ThO_2 + 5 % UO_2 + 3 % PuO_2)

(Solid lines, central fuel row; broken lines, peripheral fuel row)

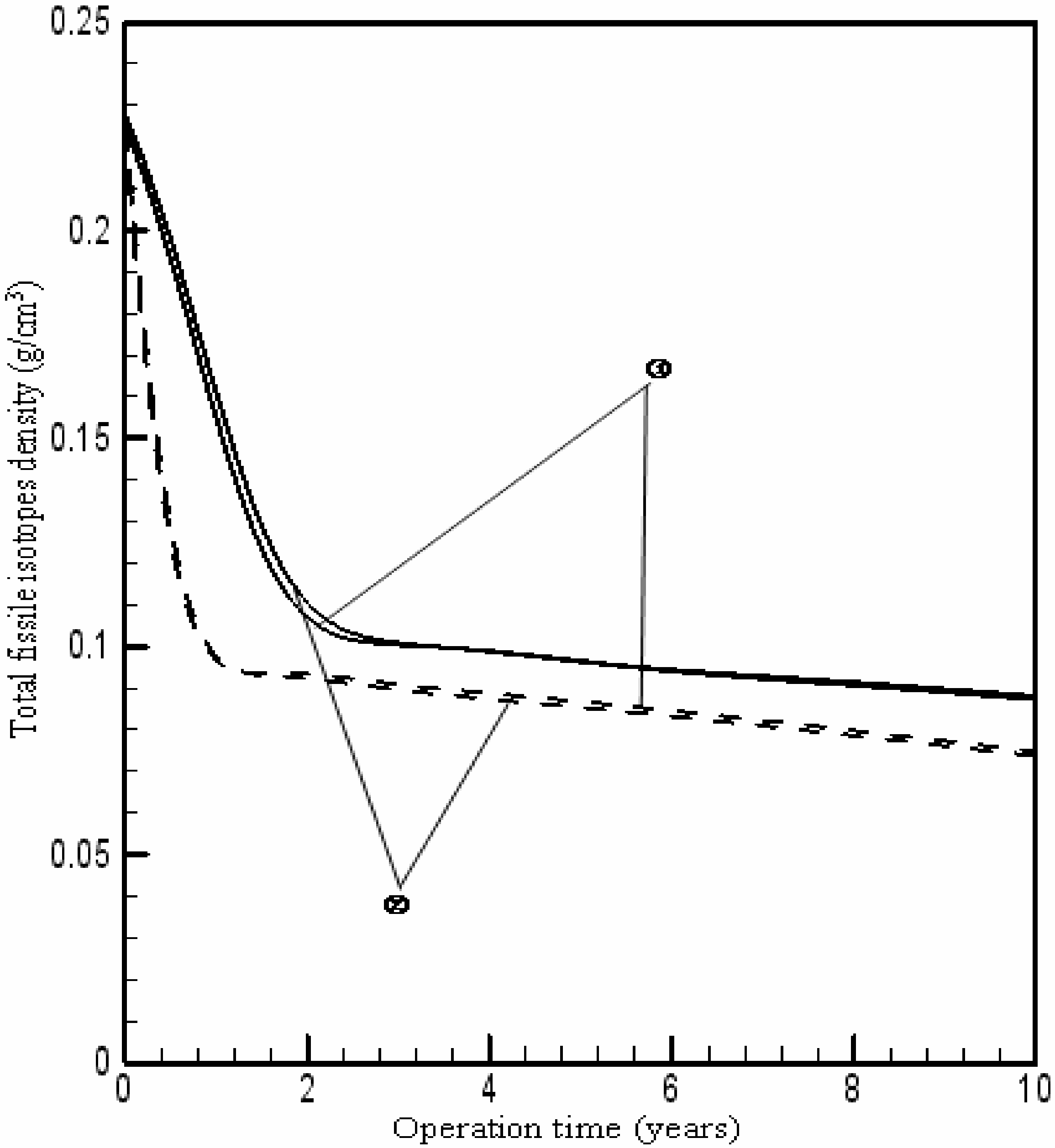

Fig. 10. Temporal variation of the accumulated densities of fissile isotopes (^{233}U+ ^{235}U+ ^{239}Pu+ ^{241}Pu) in the fuel bundle

(Legend, as fig. 9)

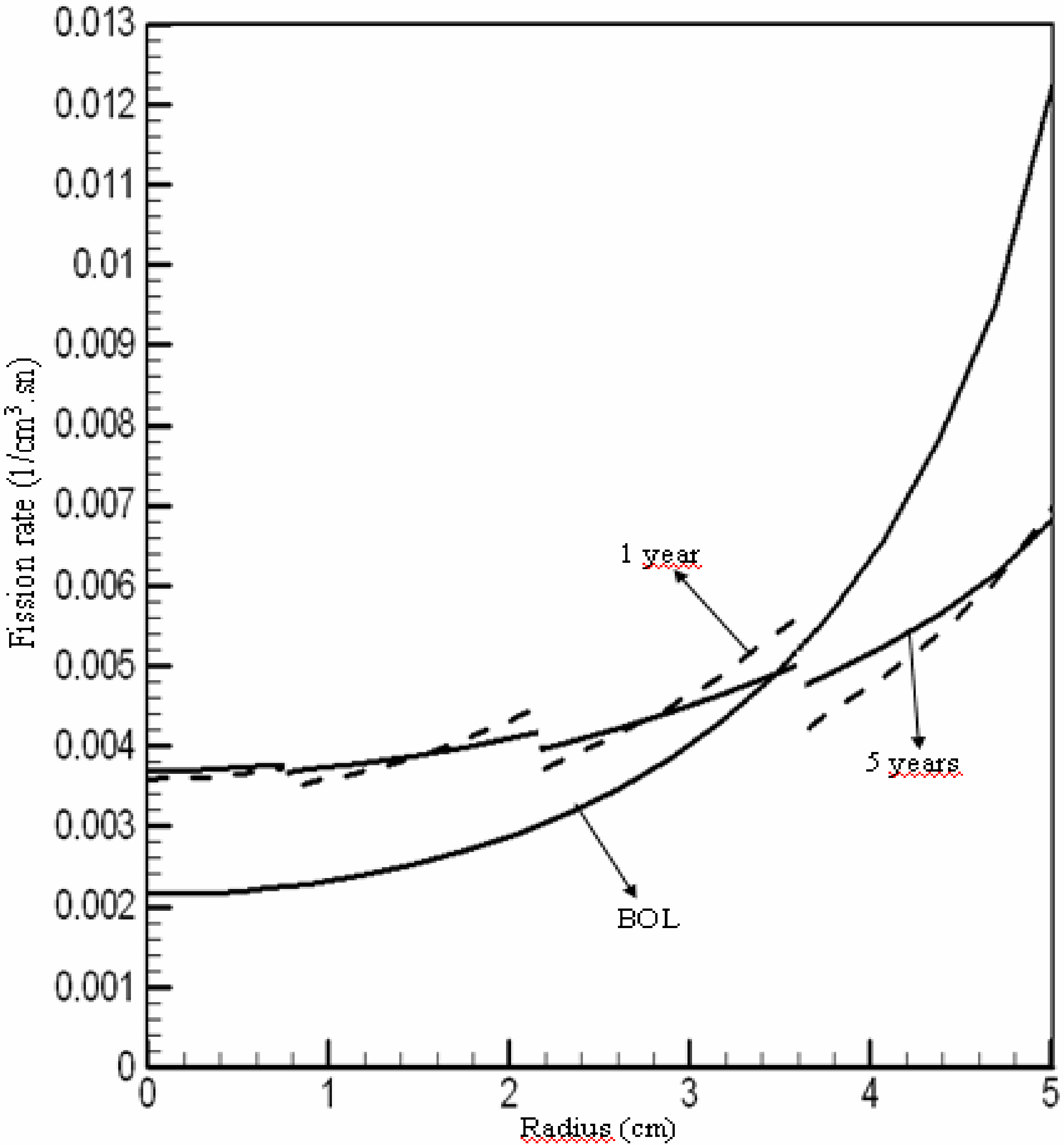

Fig. 11. Fission rate in the fuel zone of a bundle with 92 % ThO_2 + 5 % UO_2 + 3 % PuO_2

(normalized to one neutron per 1cm height)

MINOR ACTINIDE BURNING IN A CANDU THORIUM REACTOR

Table 2. The composition of the fissionable isotopes in the spent fuel

ISOTOPES	Mass (kg/year) per unit PWR[a]
^{237}Np	15.1
^{238}Pu	16.1
^{239}Pu	205
^{240}Pu	120
^{241}Pu	72.7
^{242}Pu	41.6
^{241}Am	6
^{243}Am	21.8
^{244}Cm	15.6
^{245}Cm	1.74

Pressurised-water reactor, fuel with plutonium recycle, 1000-Mwe reactor, 80% capacity factor, 33 MWd/kg, 32.5% thermal efficiency, 150 days after discharge (Nuclear Chemical Engineering, p. 370, Table 8.5).

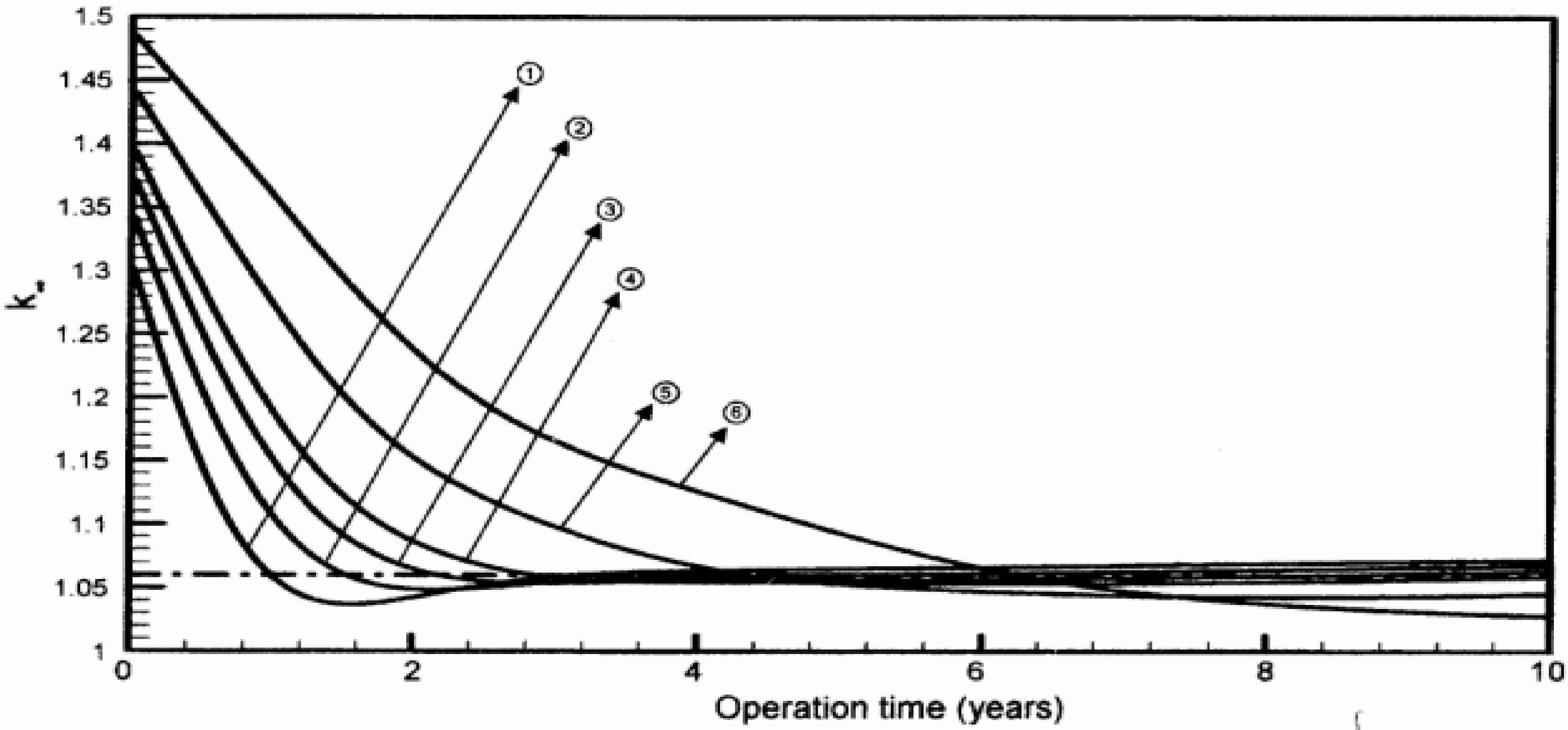

Fig. 4. Temporal variation of the lattice criticality k_∞

①: % 96 ThO_2 + % 4 MAO_2;
②: % 95 ThO_2 + % 5 MAO_2;
③: % 94 ThO_2 + % 6 MAO_2;
④: % 93 ThO_2 + % 7 MAO_2;
⑤: % 90 ThO_2 + % 10 MAO_2;
⑥: % 85 ThO_2 + % 15 MAO_2

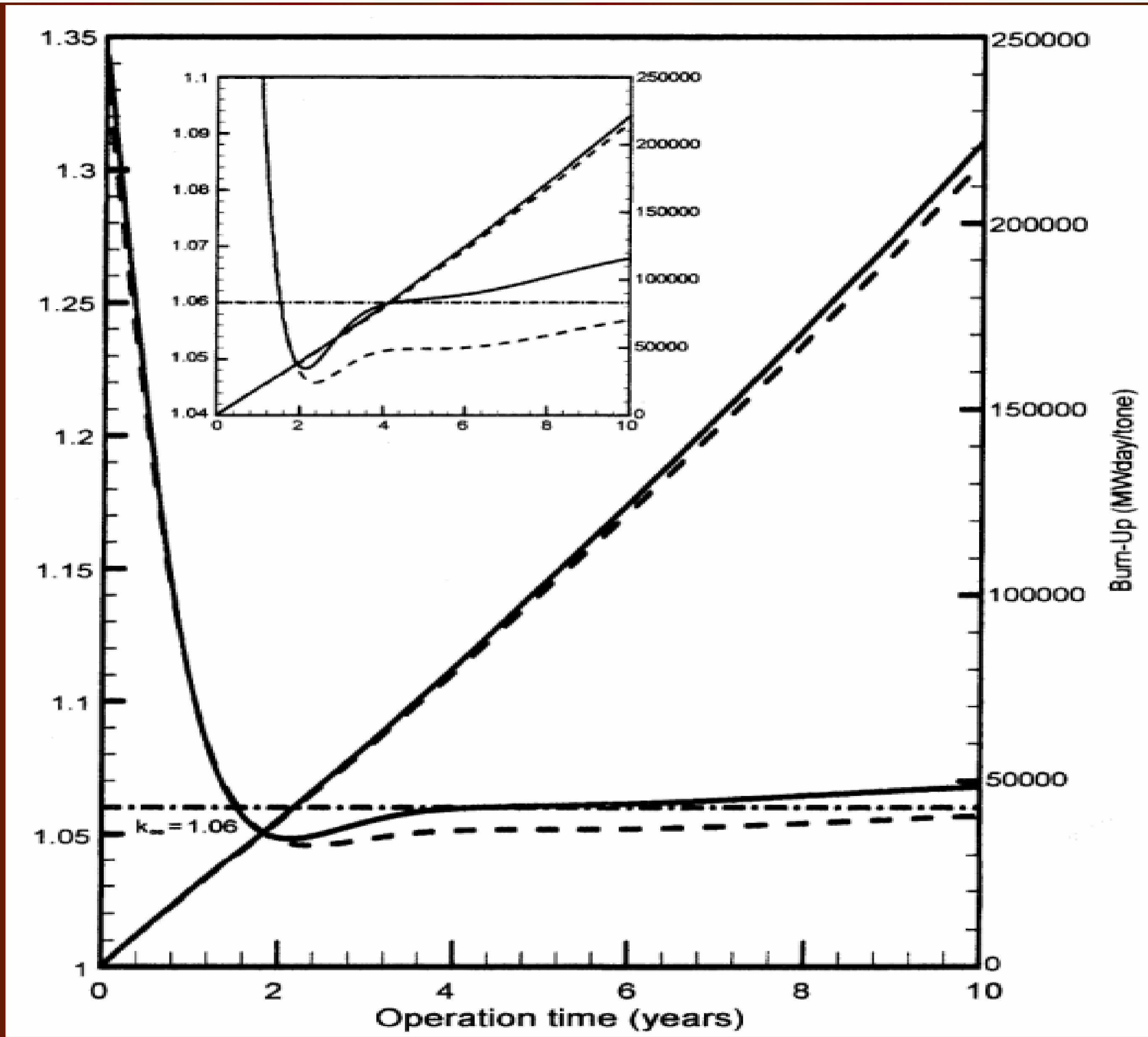

Fig 5. Temporal variation of the lattice criticality k∞ and the fuel burn-up grade

solid line: % 95 ThO2 + % 5 MAO2; dashed line: % 90 ThO2 + % 5 MAO2 + % 5 UO2

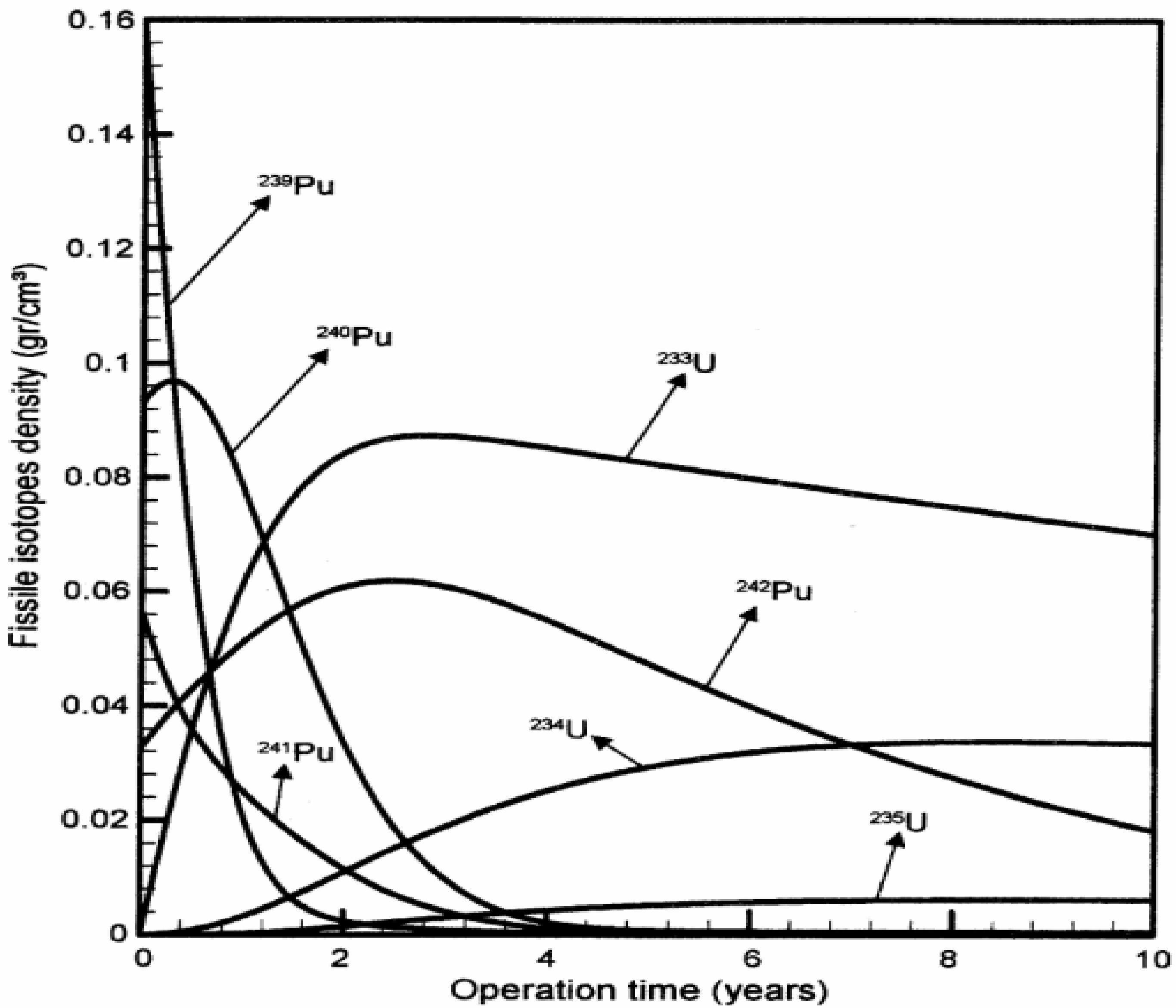

Fig 6. Density variations of the peripheral fuel row of the main fissionable isotopes in the bundle with % 95 ThO_2 + % 5 MAO_2

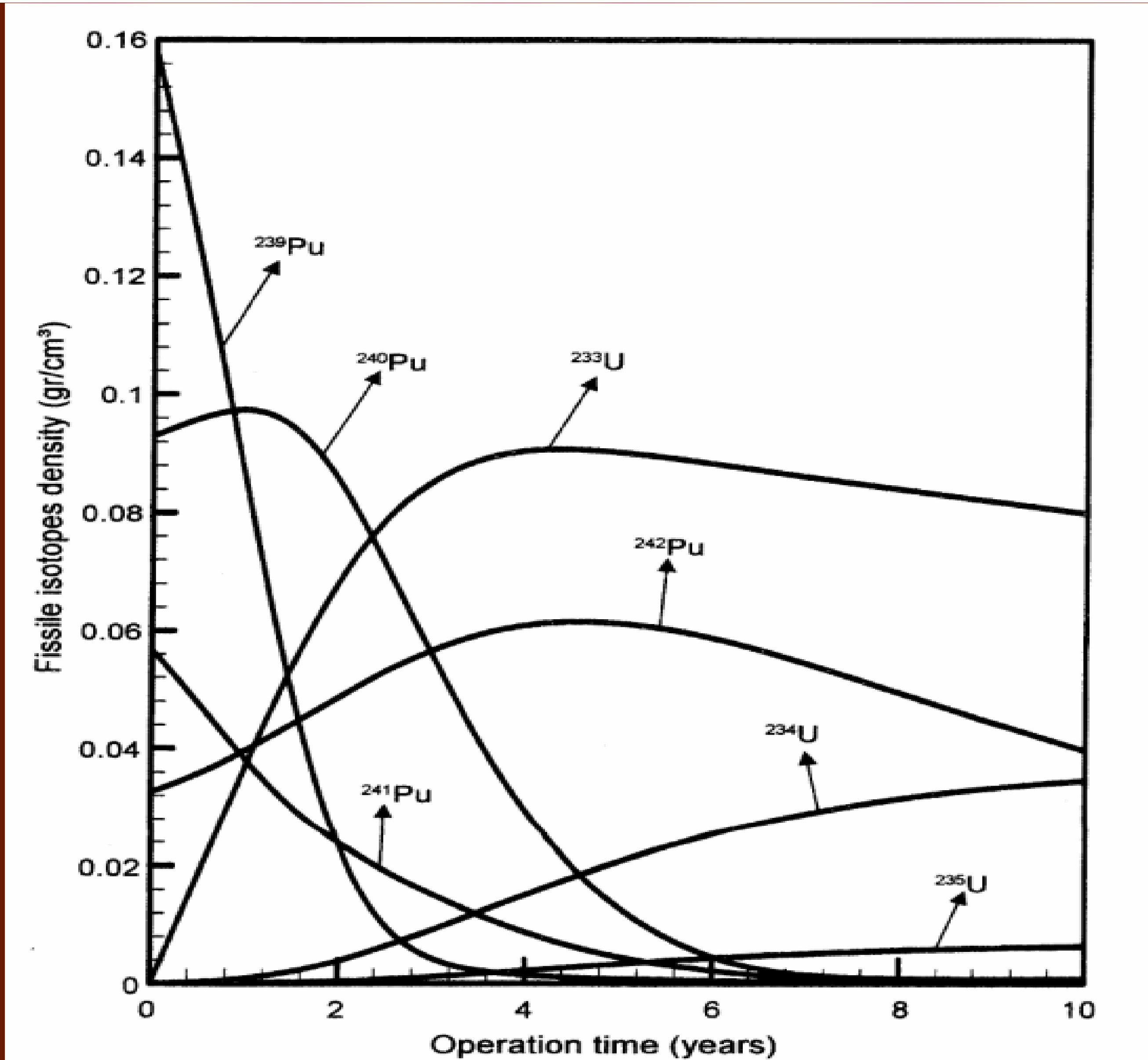

Fig 7. Density variations of the central fuel row of the main fissionable isotopes in the bundle with % 95 ThO_2 + % 5 MAO_2

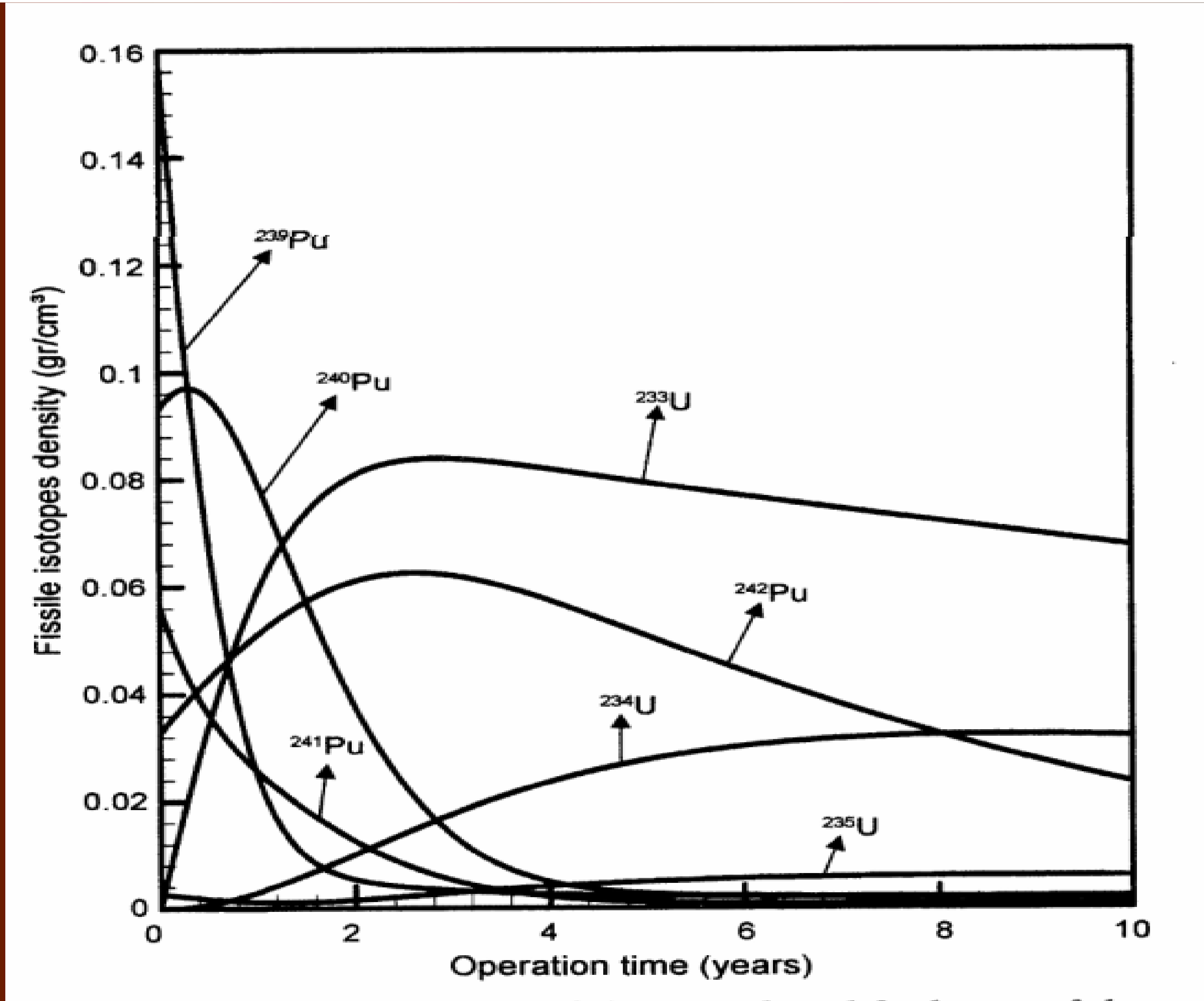

Fig 8. Density variations of the peripheral fuel row of the main fissionable isotopes in the bundle with % 90 ThO_2 + % 5 MAO_2 + % 5 UO_2

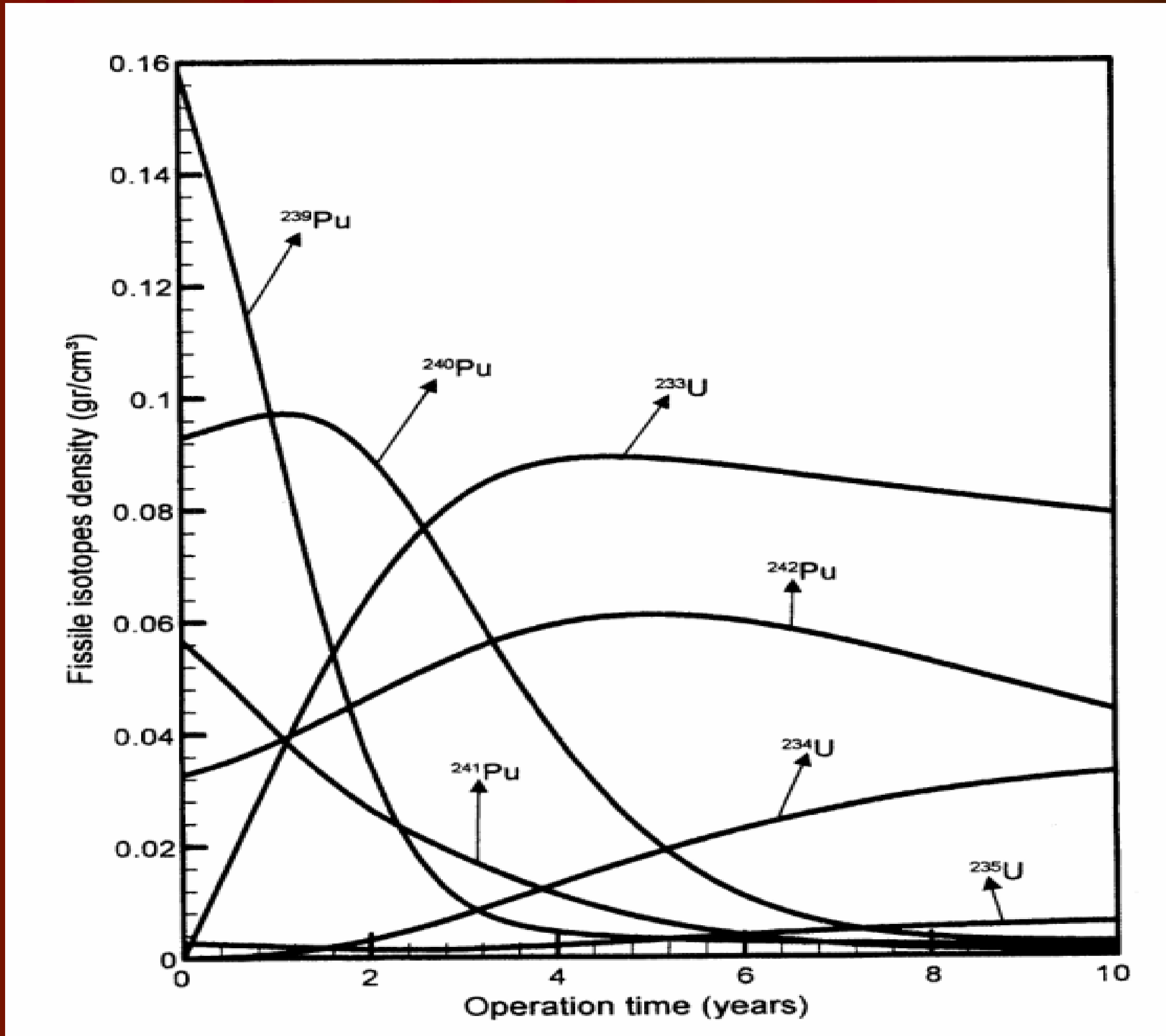

Fig 9. Density variations of the central fuel row of the main fissionable isotopes in the bundle with % 90 ThO_2 + % 5 MAO_2 + % 5 UO_2

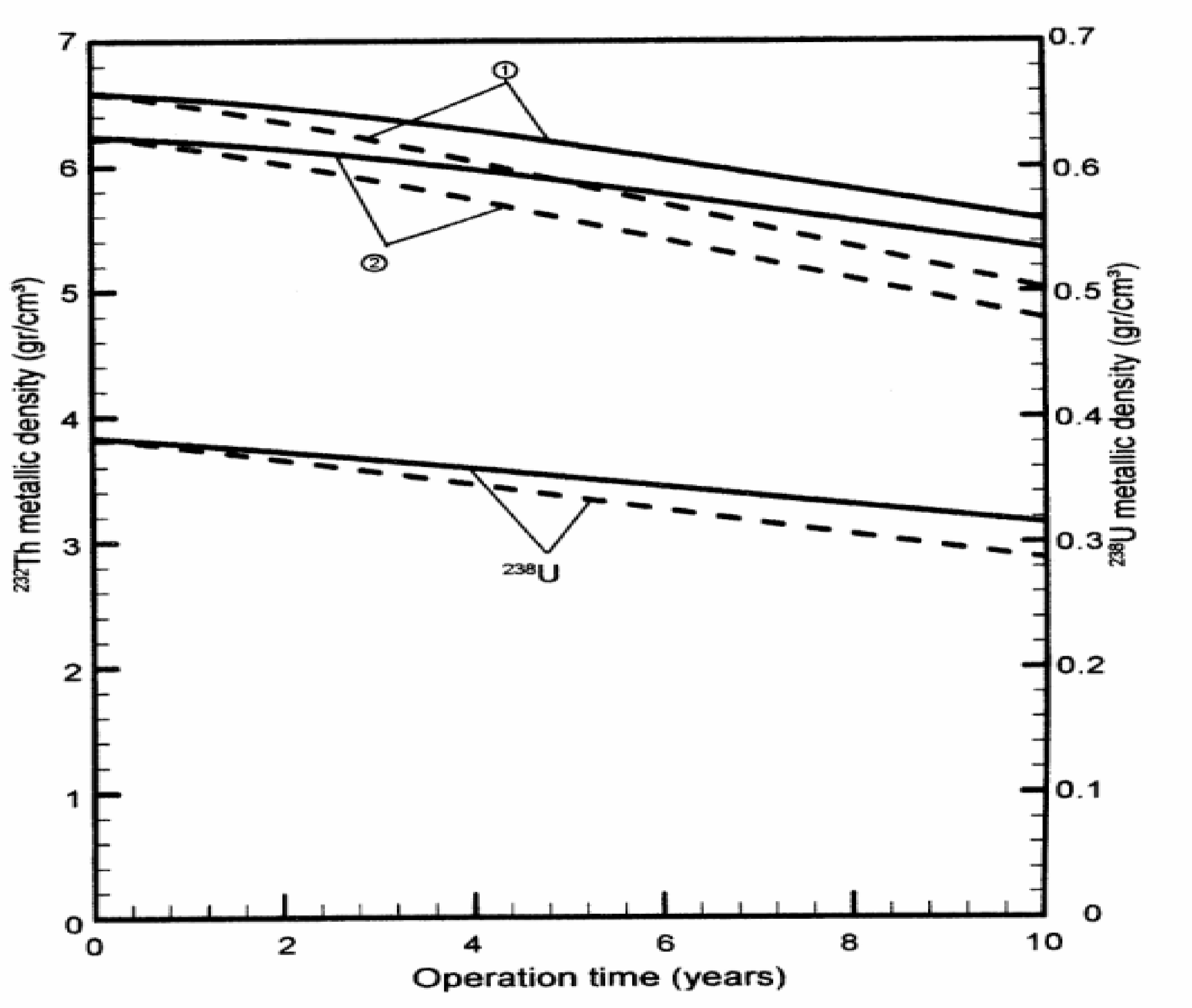

Fig 10. Gradual depletion of the metallic density of the dominant 232Th and 238U isotopes

①: % 95 ThO_2 + % 5 MAO_2 ②: % 90 ThO_2 + % 5 MAO_2 + % 5 UO_2)

(Solid lines, central fuel row; broken lines, peripheral fuel row)

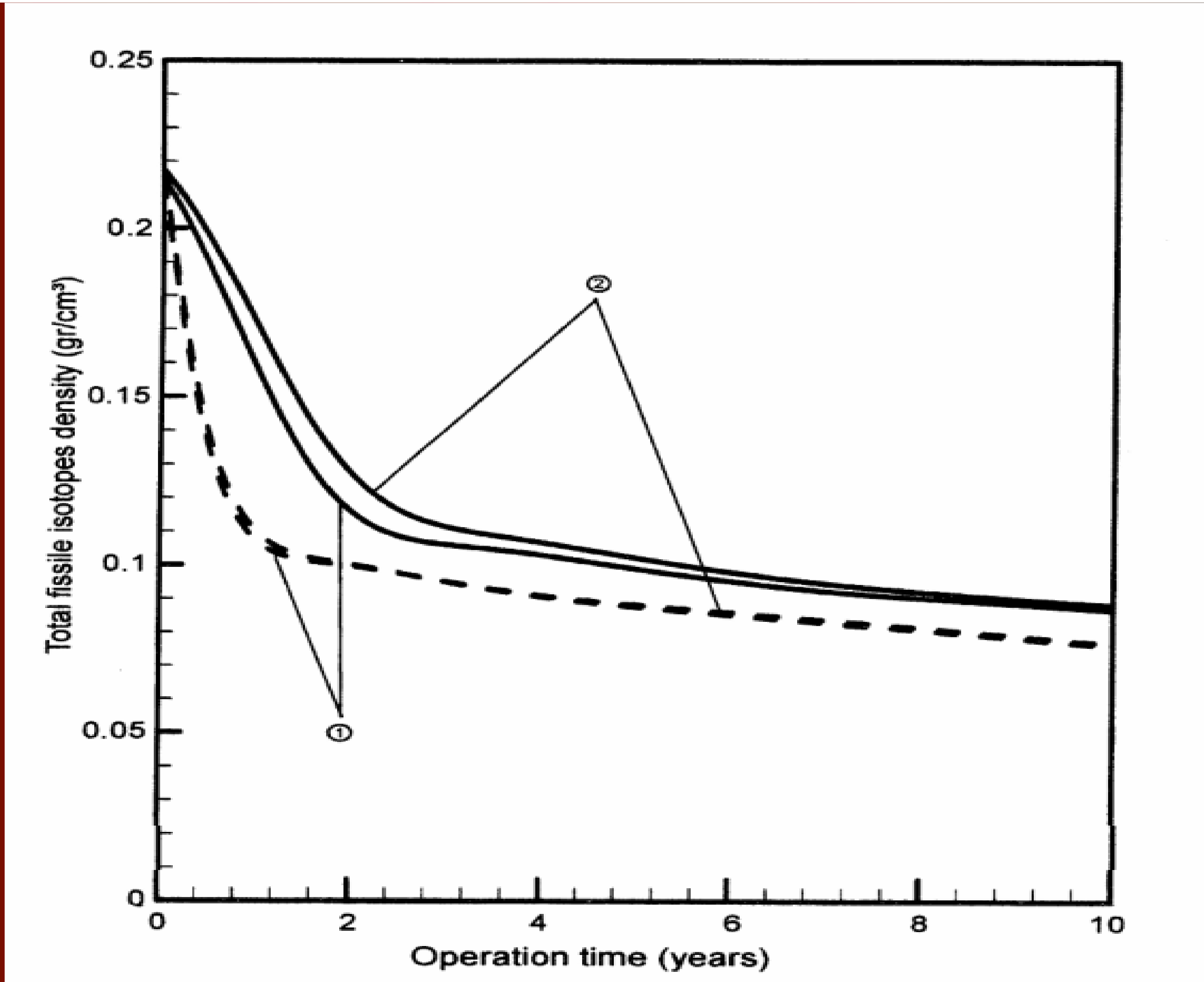

Fig 11. Temporal variation of the accumulated densities of fissile isotopes (233U+ 235U+ 239Pu+ 241Pu) in the fuel bundle

①: % 95 ThO2 + % 5 MAO2 ②: % 90 ThO2 + % 5 MAO2+ % 5 UO2)

(Solid lines, central fuel row; broken lines, peripheral fuel row)

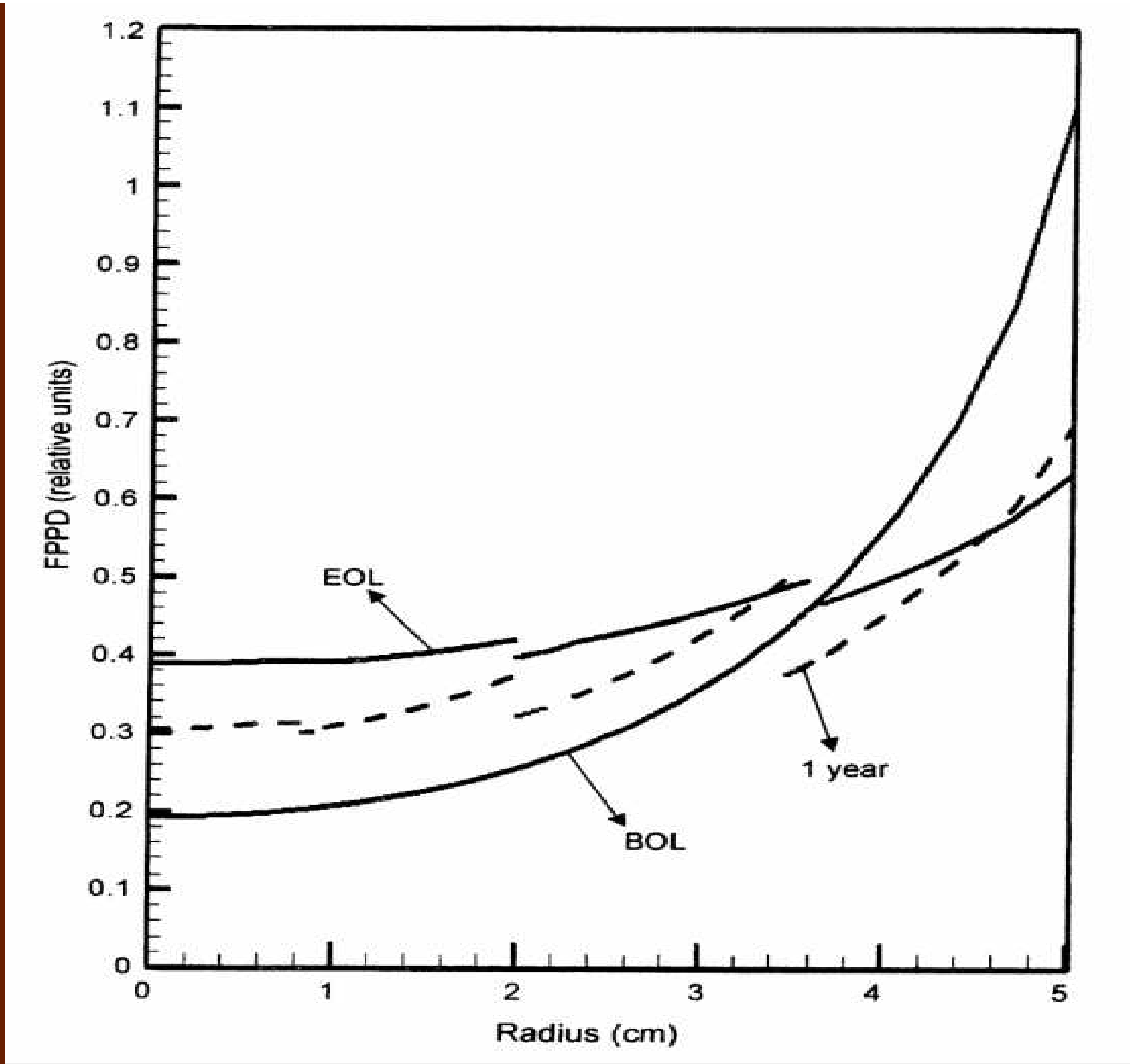

Fig 11. The fission power production density in the fuel zone of the bundle with

% 90 ThO_2 + % 5 MAO_2 + % 5 UO_2

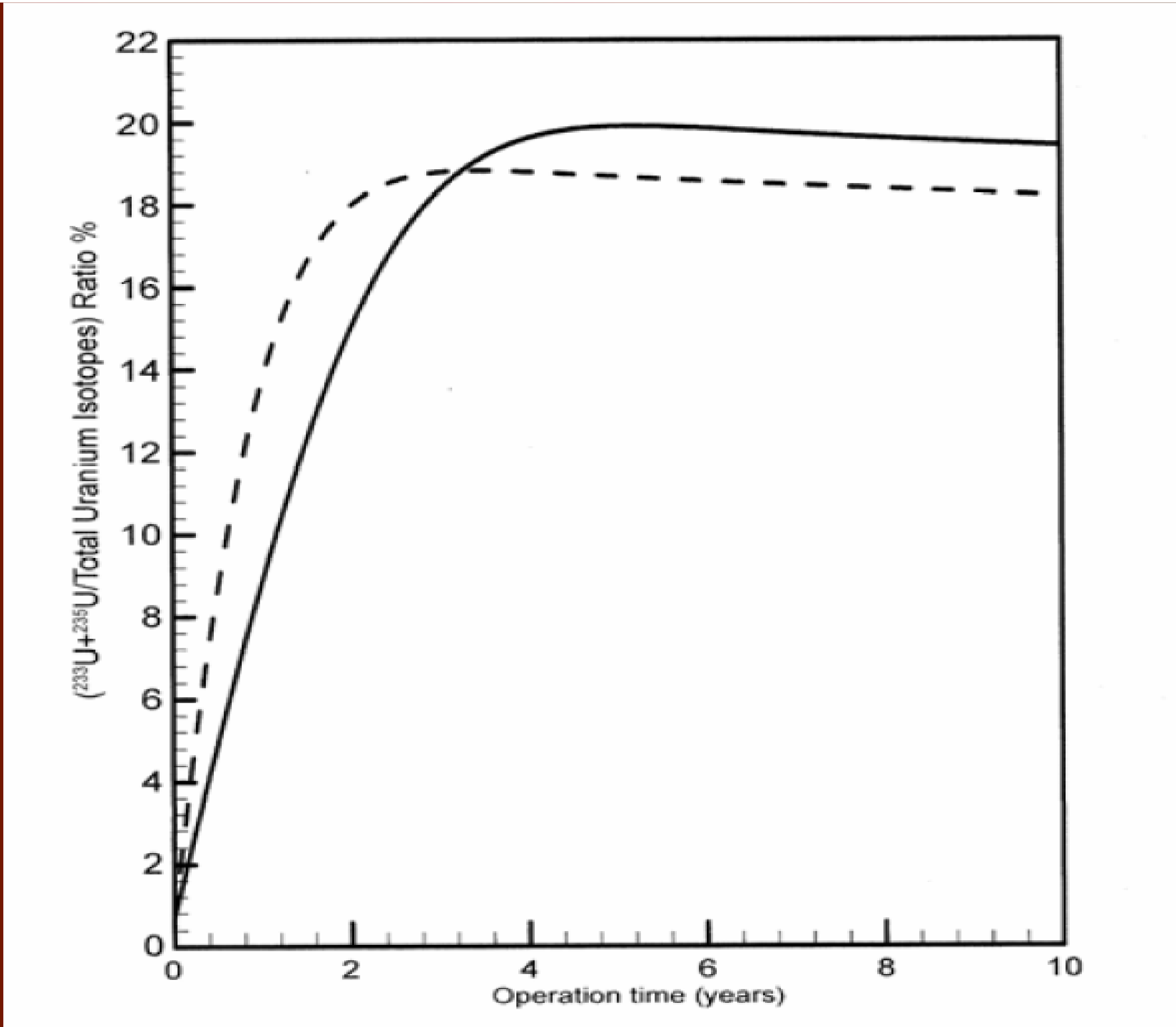

Fig 12. (233U+ 235U / Total Uranium Isotopes) ratio in the fuel bundle for % 90 ThO2 + % 5 MAO2 + % 5 UO2
(solid line: central fuel row; dashed line: peripheral fuel row)

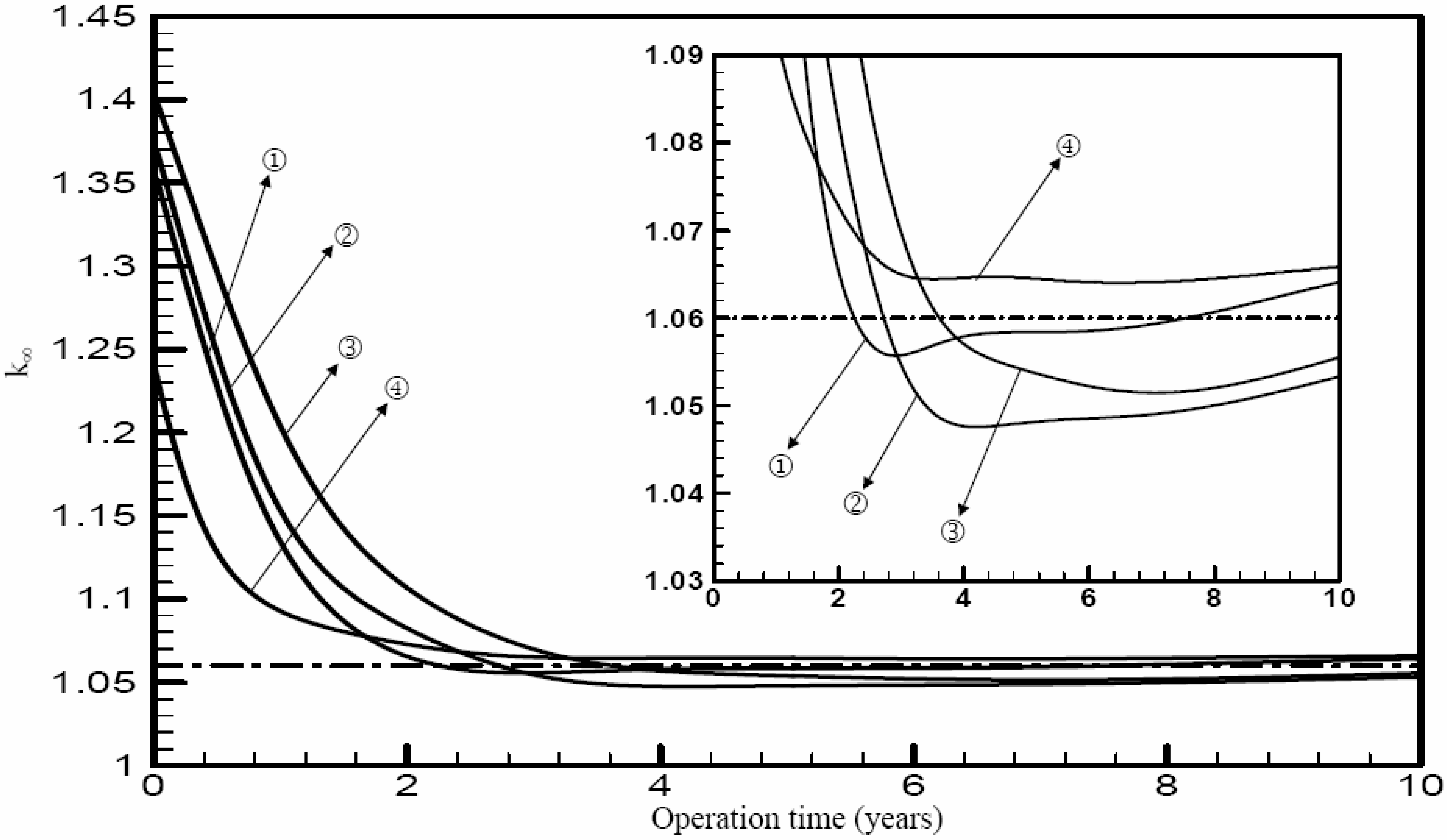

Fig. 4: Temporal variation of the lattice criticality k_∞

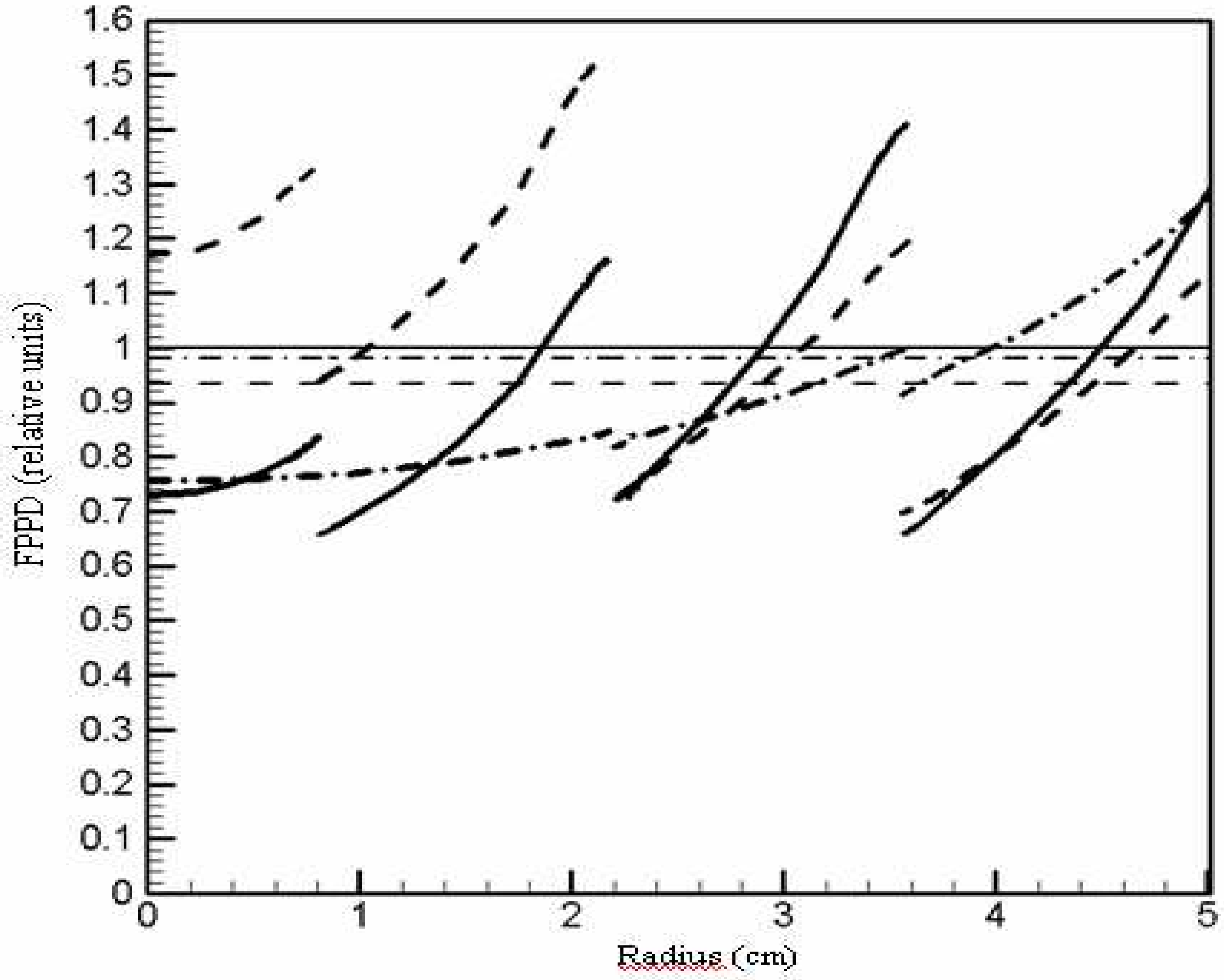

Fig.16. The fission power production density in the fuel zone of the bundle with